Deep-Sea Research II 116 (2015) 42–59

Contents lists available at ScienceDirect

Deep-Sea Research II

journal homepage: www.elsevier.com/locate/dsr2

Thorium-234 as a tracer of particle dynamics and upper ocean export in the Atlantic Ocean

S.A. Owens [a,b,*], S. Pike [a], K.O. Buesseler [a]

[a] Department of Marine Chemistry and Geochemistry MS#25, Woods Hole Oceanographic Institution, 266 Woods Hole Road, Woods Hole, MA 02543, USA
[b] MIT-WHOI Joint Program in Oceanography/Applied Ocean Science Engineering, 266 Woods Hole Road, Woods Hole, MA 02543, USA

ARTICLE INFO

Available online 12 December 2014

Keywords:
Thorium
Uranium
Particulate flux
GEOTRACES

ABSTRACT

The flux of sinking particles is an important removal mechanism of carbon and other chemical species from the surface ocean as part of the biological pump. Euphotic zone export of ^{234}Th was measured on GEOTRACES transects of the Atlantic Ocean to evaluate basin-scale export variability. High-resolution sampling through the entire water-column allowed for the identification of unique ^{234}Th features in intermediate and deep waters. These data will be important for describing distributions and estimating the fluxes of trace elements measured by other investigators in the GEOTRACES program. This extensive data set will also be useful when combined with other particulate and radioisotope data for improving our understanding of particle cycling and the relation of particle flux to particle composition and abundance.

1. Introduction

The goal of the international GEOTRACES program is to identify processes and quantify fluxes that control the distribution of trace elements and isotopes in the ocean (GEOTRACES Planning Group, 2006). Trace elements play important roles in marine biogeochemical cycles and GEOTRACES is a unique effort to quantify their role on a global scale. Isotopes are a key component of the GEOTRACES program as they can be used to measure rates of the physical, biological, and geochemical processes that determine the distribution of trace elements. Radioisotopes in particular can be used to estimate the time-scales on which these processes are important. Thorium-234 (^{234}Th), the subject of this work, can be used to determine rates of upper ocean particle export and remineralization and in combination with other isotopes of thorium, can be used to determine rates of particle aggregation and disaggregation (Waples et al., 2006). Scavenged-type trace metals, like aluminum, and nutrient-type trace metals, like iron and zinc, can be affected by the removal of particles from the surface ocean and remineralization at depth (Bruland and Lohan, 2003). Thus the rates of removal and remineralization derived from measurements of ^{234}Th are essential for understanding their distributions in the ocean.

Thorium-234 ($t_{1/2}$=24.1 d) is the particle-reactive daughter of uranium-238 (^{238}U; $t_{1/2}=4.468\times10^9$ y), which is highly soluble in seawater (Djogić et al., 1986). Due to the significantly longer half-life of ^{238}U relative to ^{234}Th, the two isotopes are in secular equilibrium (activity ^{234}Th/^{238}U=1) when there are no net removal or addition processes acting on either species. The primary use of this isotope system in the ocean has been to quantify upper ocean particle export (Bhat et al., 1969; Coale and Bruland, 1987; Buesseler et al., 1992). Particles in the surface ocean from biological production or aeolian deposition scavenge ^{234}Th. If these particles sink to deeper depths on time scales faster than ^{234}Th ingrowth, they create a deficit of ^{234}Th relative to ^{238}U (^{234}Th/^{238}U < 1) in the upper ocean. This deficit can be quantified and used to derive the flux of ^{234}Th on sinking particles. Furthermore, the sinking fluxes of other particulate species such as carbon, minerals, or trace elements can be estimated by multiplying the ^{234}Th flux and the ratio of the species of interest to ^{234}Th on the particles (Buesseler et al., 1992, 2006; Weinstein and Moran, 2005). ^{234}Th has also been used to identify regions of intense particle remineralization, often immediately below the euphotic zone, when ^{234}Th/^{238}U > 1 (Savoye et al., 2004; Buesseler et al., 2008a). ^{234}Th has been widely measured in other systems beyond the upper ocean including benthic boundary layers, surface sediments, and hydrothermal systems (Waples et al., 2006).

Much effort has been expended in the past decade to improve methods for collection and analysis of ^{234}Th in seawater. Early surveys using ^{234}Th were limited both in their spatial and depth resolution due to the large sample volume requirements. One such study, conducted on the IOC 1996 baseline metals survey, was able to identify regions of increased particle export influenced by aeolian input from the Sahara (Charette and Moran, 1999). In that

* Corresponding author at: Department of Marine Chemistry and Geochemistry MS#25, Woods Hole Oceanographic Institution, 266 Woods Hole Road, Woods Hole, MA 02543, USA.
E-mail address: stephanie.owens.morris@gmail.com (S.A. Owens).

http://dx.doi.org/10.1016/j.dsr2.2014.11.010
0967-0645/

study however, ^{234}Th species were only measured at five stations (< 10 depths/station) because each sample required ~200 L seawater. New small-volume methods require as little as 4 L of water (Benitez-Nelson et al., 2001b; Buesseler et al., 2001; Pike et al., 2005) and have been widely adopted in both process-studies and ocean transects (Buesseler et al., 2008b; Cai et al., 2008; Rutgers van der Loeff et al., 2011).

Here we present the ^{234}Th results from two transects of the Atlantic Ocean undertaken as part of the US and Dutch GEOTRACES programs in 2010 and 2011. These data are a significant contribution to the rapidly growing global ^{234}Th data set (Le Moigne et al., 2013). In this work we describe the variability in upper ocean export fluxes and derive estimates of carbon export in the Atlantic Ocean. We also highlight other interesting features of this data set including the distribution of ^{234}Th in the mid- and deep-water column and the effect of the TAG hydrothermal plume emanating from the mid-Atlantic ridge.

2. Methods

2.1. GEOTRACES cruises

Samples were collected on two U.S. GEOTRACES cruises to the North Atlantic (Section GA03) and a Dutch GEOTRACES cruise to the South Atlantic (Section GA02; Fig. 1). The first leg of the North Atlantic cruise took place on the R/V *Knorr* (KN199-4, October 15–November 4, 2010, hereafter referred to as L1) and headed due southwest from Lisbon, Portugal to 20°W, south towards the Cape Verde islands, and concluded with a four-station transect from the Mauritanian coastline (Station 9) to the ocean time-series station TENATSO (Station 12). Due to a malfunction of the ship near Station 8, the cruise was abandoned until a later date. Sampling was resumed in 2011, on the R/V *Knorr* from Woods Hole, MA to the Cape Verde islands (KN204, November 6–December 11, 2011, hereafter referred to as L2). Stations of note on the second leg included an occupation of the Bermuda Atlantic Time-series Study (BATS) site at Station 10, sampling of the TAG hydrothermal plume at Station 16, and re-occupation of the TENATSO time-series site at Station 24. On these U.S. GEOTRACES cruises, the full water column was sampled for dissolved and particulate parameters at “full” and “super” stations (denoted by filled symbols in Fig. 1). To increase spatial resolution, a subset of parameters were collected at “demi” stations (denoted by open symbols in Fig. 1) to ~1000 m.

Sampling was carried out on the Dutch GEOTRACES cruise in the South Atlantic on the RRS *James Cook* (JC057) from March 1 to April 7, 2011. Originating in Punta Arenas, Chile, the cruise track headed north from the Falkland Islands and followed the South American coastline, concluding in Gran Canaria, Spain. Full water column sampling was carried out at all “regular” and “hyper” stations for most parameters, though sampling for ^{234}Th was more limited. Particulate sampling was carried out at only six stations and was restricted to a few depths in the upper water column (denoted by filled symbols in Fig. 1).

2.2. Total ^{234}Th sampling and analyses

2.2.1. US GEOTRACES

Combined, on L1 and L2 of the US GEOTRACES cruises, 591 samples were collected for total ^{234}Th at 22 full water column stations (21 depths/station) and at 21 upper-1000 m stations (13 depths/station). Surface samples at each station were collected using a pump located in the aft hangar of the ship with a sampling pipe that extended ~1–2 m below the surface. Twelve samples in the upper ~1000 m were collected from a standard rosette and eight deeper samples were collected from Niskin bottles hung above eight *in situ* pumps. At "full" and "super" stations, 8 of the 12 shallow ^{234}Th samples matched *in situ* pump and official GEOTRACES depths. The remaining four samples were used to increase sample resolution through the upper 200 m to better define the surface ^{234}Th deficit.

2.2.2. Dutch GEOTRACES

Samples for total ^{234}Th were collected at 4 full water column stations (24 depths/station) and at 14 stations to 1000 m (13 depths/station), for a total of 276 samples. All samples were collected using the TITAN ultra-clean trace metal rosette system (De Baar et al., 2008).

2.2.3. Both cruises

Archive water samples for ^{238}U were collected concurrently with ^{234}Th samples using acid-washed vials (20 mL, 10% HCl, 5% HNO_3). Activity of ^{238}U was determined using the relationship between ^{238}U and salinity derived in Owens et al. (2011). Sampling and measurement of ^{234}Th was based on the small-volume technique originally described by Buesseler et al. (2001); deviations from this method or additional details are noted. A ^{230}Th spike (1 mL; Dutch and US L1: 2.08 ng g^{-1}; US L2: 1.05 ng g^{-1}) was added to each sample using a calibrated repeater pipette and samples were allowed to equilibrate for 7–8 h.

In preparation for beta counting, filters were placed on plastic mounts and covered with a single layer of Mylar and a double layer of aluminum foil. All samples were counted at sea on RISØ Laboratories anti-coincidence beta counters for 12 h; samples were counted a second time and the mean value of two counts, decay corrected to collection time are reported here. Samples were recounted 5–6 months later to determine background radioactivity due to beta decay of long lived natural radionuclides that are also carried by the Mn precipitate. At the start and conclusion of each cruise, low and high activity ^{238}U standards and background counts were measured to confirm correct operation of the RISØ detectors. On the US cruises, a helium/1% butane mixture was used for quench gas in the detectors and on the Dutch cruise, an argon/1% isobutane mixture was used.

After samples were counted for a final time, they were prepared for ICP–MS to determine the percent recovery of the ^{230}Th spike and thus chemical yield of ^{234}Th in the Mn precipitate. The method used here was adapted from that of Pike et al. (2005); here, the samples were not purified using column chemistry techniques. Briefly, the samples were leached, spiked with a ^{229}Th tracer, equilibrated overnight, and then diluted before analysis by ICP–MS. The mean sample recovery for typical samples, those that were not noted as having broken filters or visibly lost material, was 88%. The beta detectors' efficiency for this method was determined using ^{234}Th data between 1000 m and 1000 m above the bottom, where equilibrium between ^{238}U and ^{234}Th is expected, and minimizing the percent difference between the mean values of ^{238}U and ^{234}Th.

2.3. Particulate ^{234}Th and carbon sampling and analyses

2.3.1. US GEOTRACES

Particulate ^{234}Th samples were collected using McLane *in situ* pumps modified to accommodate two filter heads (Morris et al., 2011). At “full” and “super” stations, in situ pumps were deployed at 16 depths that matched total ^{234}Th depths. Both filter heads contained 51 μm pre-filters (Lam et al., 2015). Below these pre-filters, one filter head contained a Supor filter and the other contained a precombusted and acid-leached QMA filter. Particles from half of the Supor pre-filter on L1 and the whole Supor pre-filter on L2 were rinsed onto silver filters using 1.0 μm-filtered

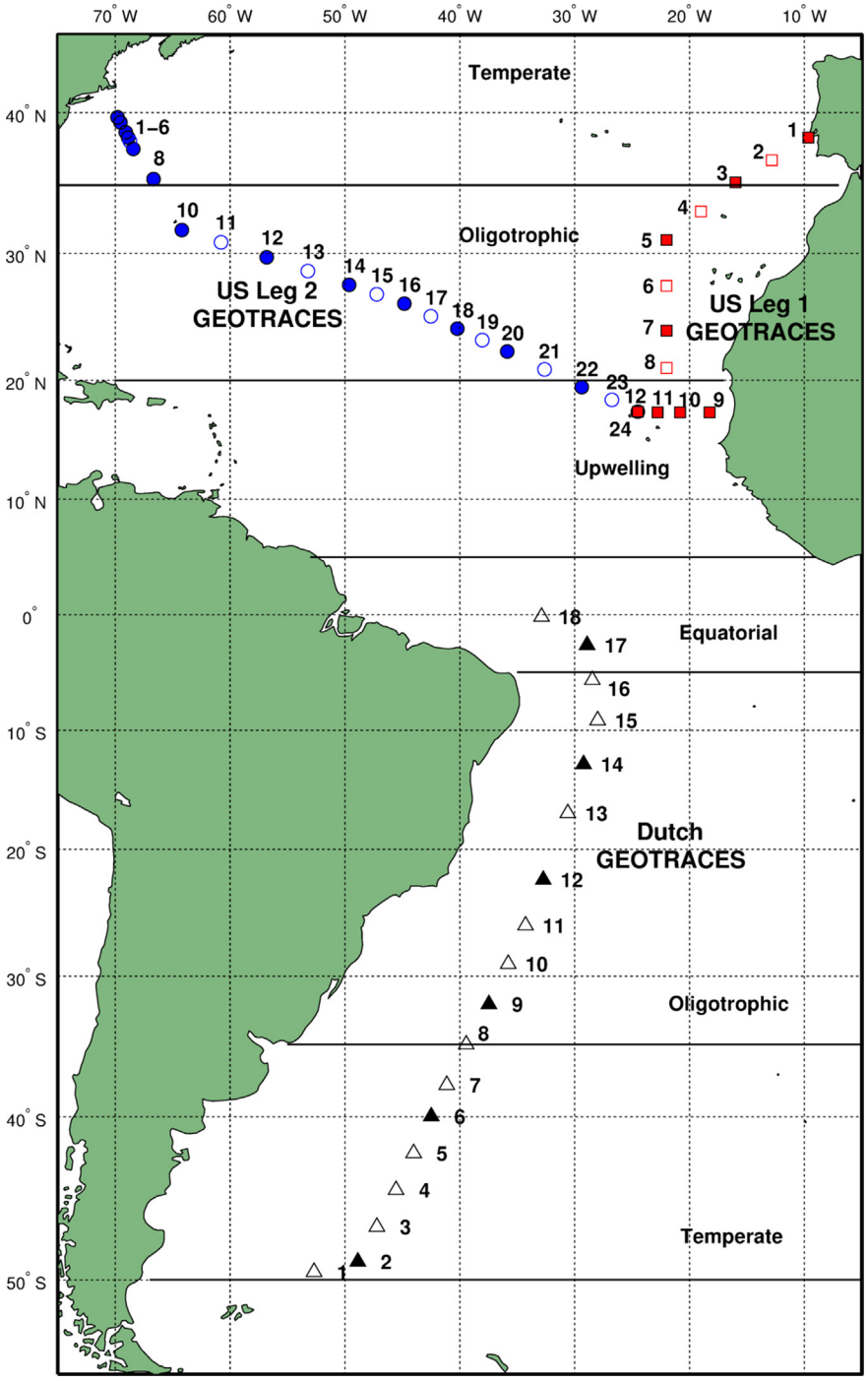

Fig. 1. Sampling locations from Atlantic GEOTRACES campaigns. The northern Atlantic transect was sampled in two parts in October/November 2010 (red) and November/December 2011 (blue). The southern Atlantic was sampled in March/April 2011 (black). Filled symbols are where total and particulate ^{234}Th were sampled and hollow symbols are where only total ^{234}Th was sampled. (For interpretation of the references to color in this figure legend, the reader is referred to the web version of this article.)

seawater. The volume pumped through each pre-filter and QMA was determined from flow meters mounted below each filter head; the mean volume pumped through each whole Supor pre-filter was 475 L. The whole QMAs were oven dried and then a 25 mm-diameter subsample was taken for beta counting. The mean effective volume for the 25 mm QMA subsample was 47 L. The >51 μm samples from the pre-filters were also oven-dried and both sets of samples were prepared for beta counting as described for total ^{234}Th samples above. Additional 12 mm punches were taken from the whole QMA for determination of total carbon. These 12 mm punches and subsamples of the Ag filters were analyzed for total carbon using a ThermoQuest Flash EA112 Carbon/Nitrogen Analyzer and blank corrected based on a dipped blank (Lam et al., 2015). Particulate inorganic carbon (PIC) analyses are also being carried out on these samples by the P.J. Lam group and will be available at a later date in order to determine particulate organic carbon (POC) by difference (POC=Total C−PIC). In the upper 200 m of the regions sampled on this cruise, PIC is likely often less than 10% of the total C or within the error of the ^{234}Th-derived C fluxes.

2.3.2. Dutch GEOTRACES

In situ pumps were deployed at three depths between 50 and 200 m at six stations with one filter head, containing only a 51 μm pre-filter. Pump deployment times were ~30 min and the mean pumped volume was ~450 L. Particles were rinsed onto silver filters, oven-dried, and beta counted using RISØ detectors. The silver filters were subsampled and analyzed only for total carbon.

3. Results and discussion

3.1. Particle export and remineralization in the upper ocean

3.1.1. Calculating ^{234}Th export from the upper ocean

The primary use of the ^{234}Th/^{238}U disequilibrium method has been for determining particle export from the upper water column, a key pathway in the biological carbon pump and a conduit for scavenging removal of trace elements. To determine this export flux, it is necessary to define the surface deficit of ^{234}Th as well as possible (Figs. 2–4). To calculate the flux of ^{234}Th, an expression of ^{234}Th activity with time (∂^{234}Th/∂t) is required:

$$\frac{\partial^{234}\mathrm{Th}}{\partial t} = (^{238}\mathrm{U} - ^{234}\mathrm{Th})\lambda - P + V$$

where ^{238}U is the activity of uranium, ^{234}Th is the measured activity of total ^{234}Th, λ is the decay constant of ^{234}Th (0.0288 day^{-1}), V is the sum of advective and vertical diffusive fluxes of ^{234}Th, and P is the export of ^{234}Th on sinking particles. Here we assume that ∂^{234}Th/∂t equals zero or that the system is in steady state. A non-steady state model would require measurements of ^{234}Th profiles every few days to weeks at the same site, which is not possible on these transect cruises (Savoye et al., 2006). Non-steady state effects are most important in periods of significant ^{234}Th change such as during or at the end of phytoplankton blooms (Buesseler et al., 1992; Charette and Buesseler, 2000). Thus, the assumption of steady state will introduce greater uncertainty into the flux calculations if any of the measurements presented here coincide with rapid changes in ^{234}Th.

Typically, the role of horizontal and vertical transport processes of ^{234}Th, other than export, are not considered because of their minor contribution relative to the downward flux and the uncertainty of these flux estimates (Savoye et al., 2006; Cai et al., 2008). This is a reasonable assumption for the majority of the stations sampled on these cruises, as concluded in prior studies (Thomalla et al., 2006; Buesseler et al., 2008a; Resplandy et al., 2012). This assumption may not hold in regions such as the Gulf Stream, sampled on L2, and the upwelling region off the coast of Mauritania, sampled on L1. In the Gulf Stream, lateral transport of ^{234}Th may be important however, the gradient in the direction of the Gulf Stream was not sampled and thus we cannot evaluate this assumption here. Off the coast of Mauritania, winds drive coastal water offshore and very close to the coast, water upwells to compensate (Mittelstaedt, 1991). Here we can

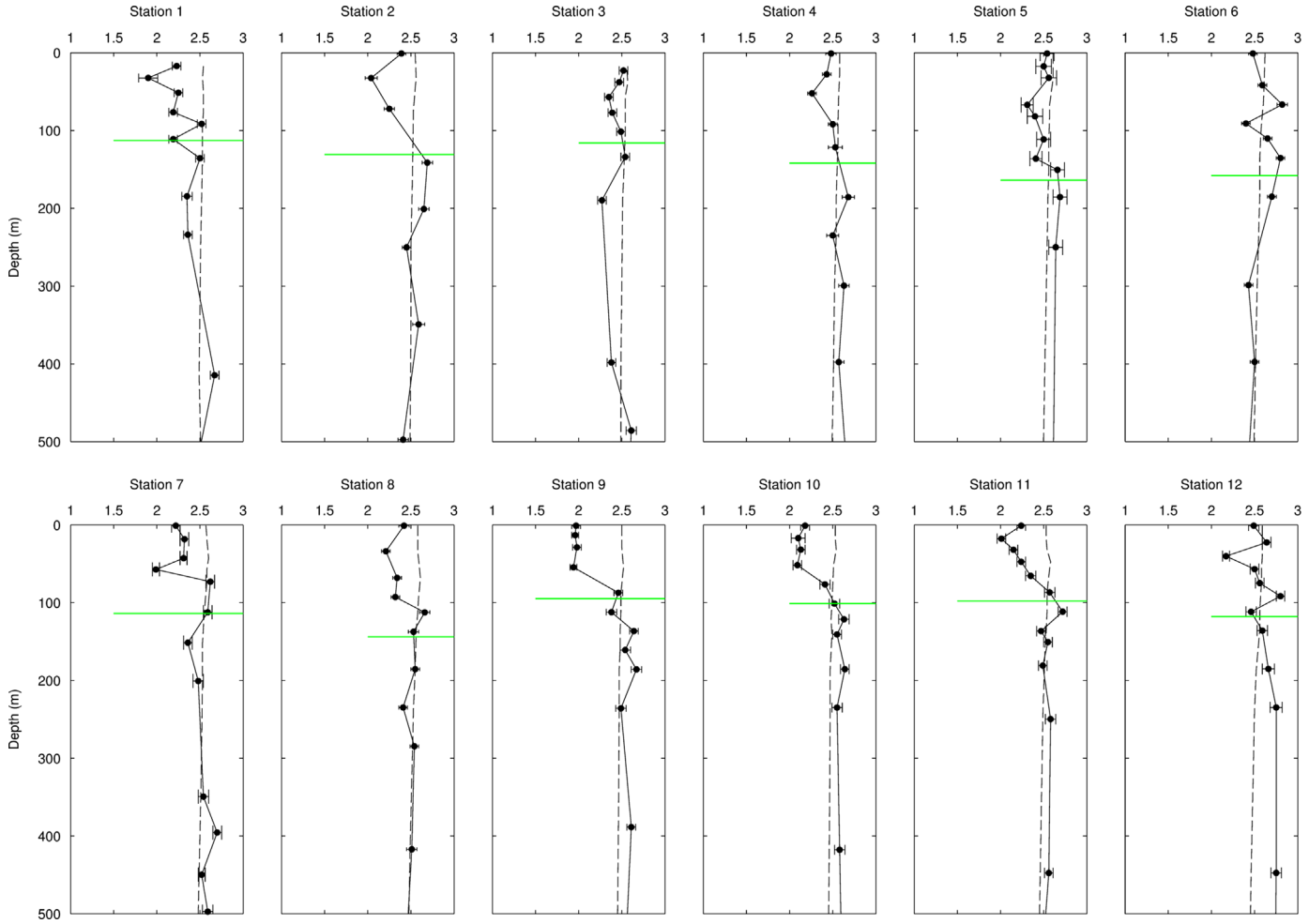

Fig. 2. ^{234}Th profiles in the upper 500 m of the water column from US GEOTRACES Leg 1 (locations in red, Fig. 1). The vertical dashed line is ^{238}U activity and the horizontal green line is the calculated PPZ depth. The same convention for ^{238}U and ^{234}Th is used throughout these figures. (For interpretation of the references to color in this figure legend, the reader is referred to the web version of this article.)

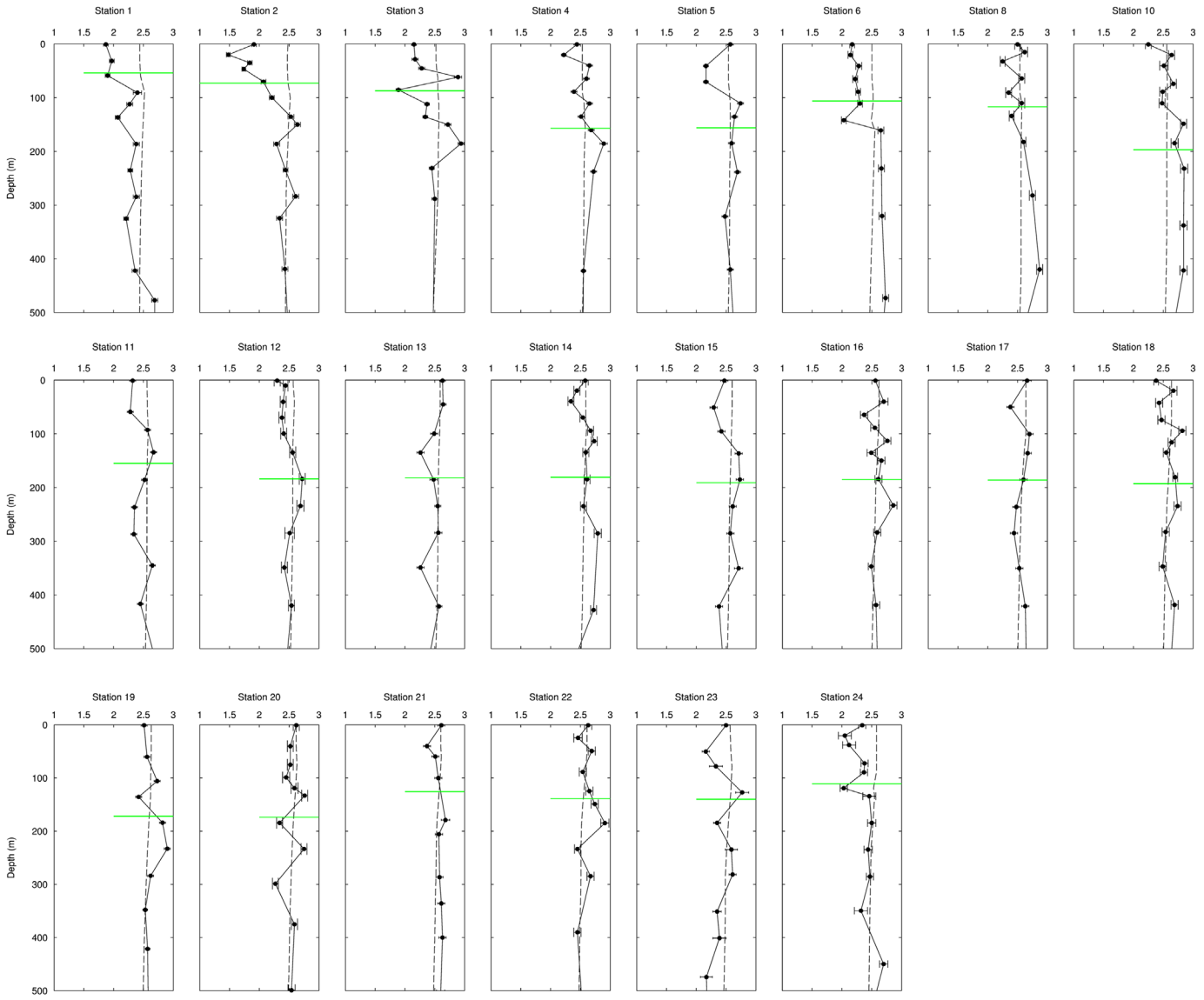

Fig. 3. ^{234}Th profiles in the upper 500 m of the water column from US GEOTRACES Leg 2 (in blue, Fig. 1). (For interpretation of the references to color in this figure legend, the reader is referred to the web version of this article.)

estimate the effects of not including offshore advection and vertical diffusivity in our flux calculations. On L1, there was a small offshore gradient from Stations 9 to 12 of increasing ^{234}Th activity in the upper 100 m of 0.0007 dpm L^{-1} km^{-1}. Assuming an advection rate of 4 cm s^{-1} (Mittelstaedt, 1991), this translates to a ^{234}Th flux of 245 dpm m^{-2} d^{-1} or the amount by which ^{234}Th export at the offshore stations would be overestimated. Vertical diffusivity rates from this cruise have been estimated using ^{228}Ra (Morris et al., 2012) and range from 0.33 to 0.88 cm^2 s^{-1}. Using the maximum estimate of diffusivity rates and the maximum gradient in ^{234}Th from Station 9 (0.52 dpm L^{-1} m^{-1}), vertical diffusion of ^{234}Th is on the order of 75 dpm m^{-2} d^{-1}, which is less than the uncertainty on the downward ^{234}Th flux estimates. At present, we assume that horizontal and vertical processes are not significant in the ^{234}Th budget relative to the downward flux. In the future however, when additional tracer information from these GEOTRACES cruises is available, we may be able to improve our model by incorporating these processes.

3.1.2. *Integration depth for export calculations*

Many prior uses of ^{234}Th to determine particle fluxes have used a single fixed integration depth, either for convenience, because of limited sampling resolution in the surface ocean, or because a single depth reasonably defined the depth where ^{234}Th and ^{238}U were in equilibrium. More recently however, Buesseler and Boyd (2009) have shown that using a single depth can bias temporal or spatial comparisons of particle export and biological pump strength. They determined that a more appropriate method is to integrate to the depth where net primary production goes to zero when making comparisons between the production of POC via autotrophy, and the export efficiency of POC from the euphotic zone. In the case of the data sets they analyzed, they chose to integrate to the depth of the 1% light level. Thus, different regions of the upper ocean could be compared across seasons and regions to each other in terms of the biological pump strength. For particle reactive trace elements and isotopes (TEIs) the same principle would apply; in the euphotic zone new particle surfaces would be created, and below the euphotic zone, suspended and sinking particles would only be recycled via physical and biological processes that in general, lead to the attenuation of export of TEIs on sinking particles.

The GEOTRACES transects presented in this work span diverse biogeographic regions and thus a single fixed depth is unlikely to accurately describe the region of the upper ocean where primary

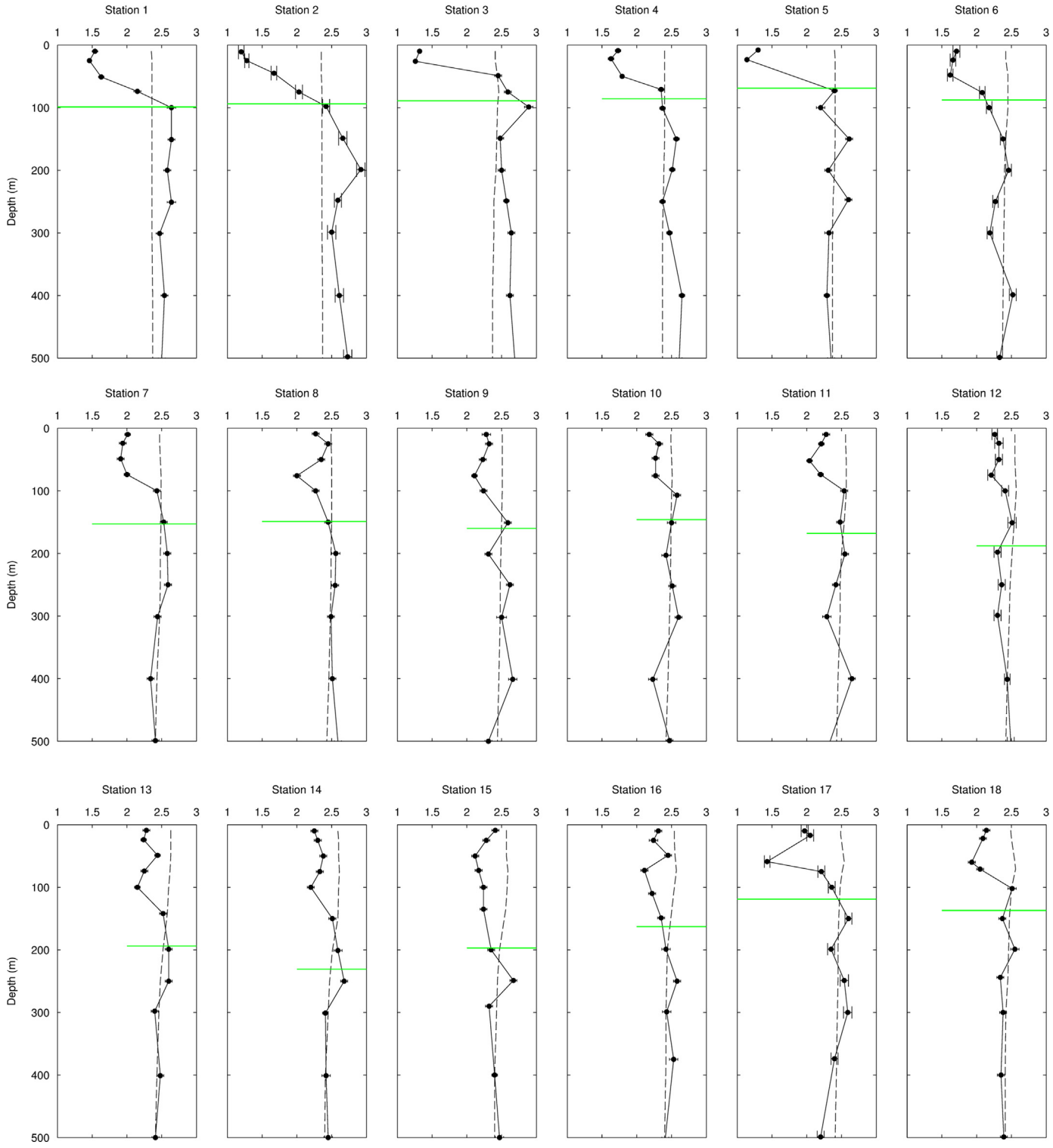

Fig. 4. ^{234}Th profiles in the upper 500 m of the water column from the South Atlantic Dutch GEOTRACES campaign (in black, Fig. 1).

production is occurring at each station. There were not photosynthetically available radiation (PAR) or other light sensors on board the GEOTRACES deployment instruments, thus light data were not able to derive an integration depth. Transmissometry data could have been used to define the particle-rich surface zone; however, other processes such as lateral input of particles and particle size would influence this parameter at various depths in the water column. Fluorescence was chosen as the integration depth-defining parameter as it was available across all of the cruises and is related, although, non-linearly to the amount of primary production occurring in the water column. As another alternative, the ^{234}Th–^{238}U equilibrium depth could have been chosen as the integration depth, however this method is different in that there can be deficits below or shallower than the euphotic zone, and it is often difficult to constrain the exact depth of equilibrium given the low number of data points across this depth region.

Here we define this primary production zone (PPZ) as the region from 0 m to the depth at which the fluorescence reaches 10% of its maximum value. We have chosen to err on the conservative or shallow side (Figs. 2–4). The use of the PPZ as defined here is corroborated by recent work by Marra et al. (2014), who showed that the base of the euphotic zone or the compensation depth, where net primary production goes to zero and phytoplankton respiration and gross primary production are equal, to often be deeper than the 1% light level, the frequently-used definition for the euphotic zone. The difference between the measured compensation depths and the depth of the 1% light level was meters to tens of meters deeper. Additionally, they found that the compensation depths appeared to encompass the entire depth range of autotrophic biomass and were thus located deeper than the deep chlorophyll maximum, as approximated by the PPZ definition used here.

The light- versus fluorescence-based calculations cannot be compared here because of the absence of any light data. However, to demonstrate the utility of the PPZ definition in an alternate location, Fig. 5 shows temperature, salinity, light, fluorescence, and transmissometer profiles from a sampling program off the West Antarctic Peninsula where data from all of these sensors was available. In this example, the PPZ encompasses the region over which fluorescence is elevated (center panel) and light transmission is decreased (right panel) better than the 1% light level definition of the euphotic zone. Off the West Antarctic Peninsula, over a large area and several months, the mean PPZ depth was approximately 35 to 40 m deeper than the mean 1% light level; ^{234}Th fluxes at the 1% light level accounted for only ~75% of the ^{234}Th flux at the base of the PPZ. From the GEOTRACES cruises, Fig. 6 demonstrates the use of the PPZ at L1 stations. It is important to note, that if 100 m was chosen as the integration depth for all these stations, significant parts of the PPZ would be below our depth of integration, particularly at Stations 4, 5, 6, and 8 where 100 m is near to the depth of the chlorophyll maximum. To compare this data set to prior studies and other GEOTRACES data sets however, we have provided ^{234}Th flux both at the base of the PPZ and at 100 m (Table 1). Other particulate TEI's fluxes can thus be calculated using either depth horizon and the particulate TEI/^{234}Th ratio at the appropriate depth.

3.1.3. *Carbon to ^{234}Th ratios of large "sinking" particles*

Carbon to ^{234}Th ratios (C/^{234}Th) on sinking particles, which are operationally defined here as >51 μm (Bishop et al., 1977; Lam et al., 2015), can be multiplied by the ^{234}Th fluxes at the PPZ to derive estimates of carbon export. Particulate sampling was carried out at a subset of the stations where total ^{234}Th was measured, thus site-specific C/^{234}Th ratios at the PPZ are not available for every station. Consistent with previous studies (Buesseler et al., 2006), across all stations, C/^{234}Th ratios were highest in the surface and at the margins and decreased with depth (Fig. 7). Below 100 m, there was little variability in C/^{234}Th ratios despite the large area and diverse regions measured in this study (Figs. 7 and 8). Only samples from Station 1 in the northeast Atlantic at 185 and 235 m deviated from the general trend due to very low particulate ^{234}Th values at these depths.

To obtain C/^{234}Th ratios at the PPZ depth at each site, data between 70 and 250 m (except L1 Station 1 samples) were sorted into 20 m bins and averaged. A power law relationship was derived using these values (Fig. 8) and C/^{234}Th ratios at the PPZ were calculated for each site (Table 1). For L1 Station 1, a site-

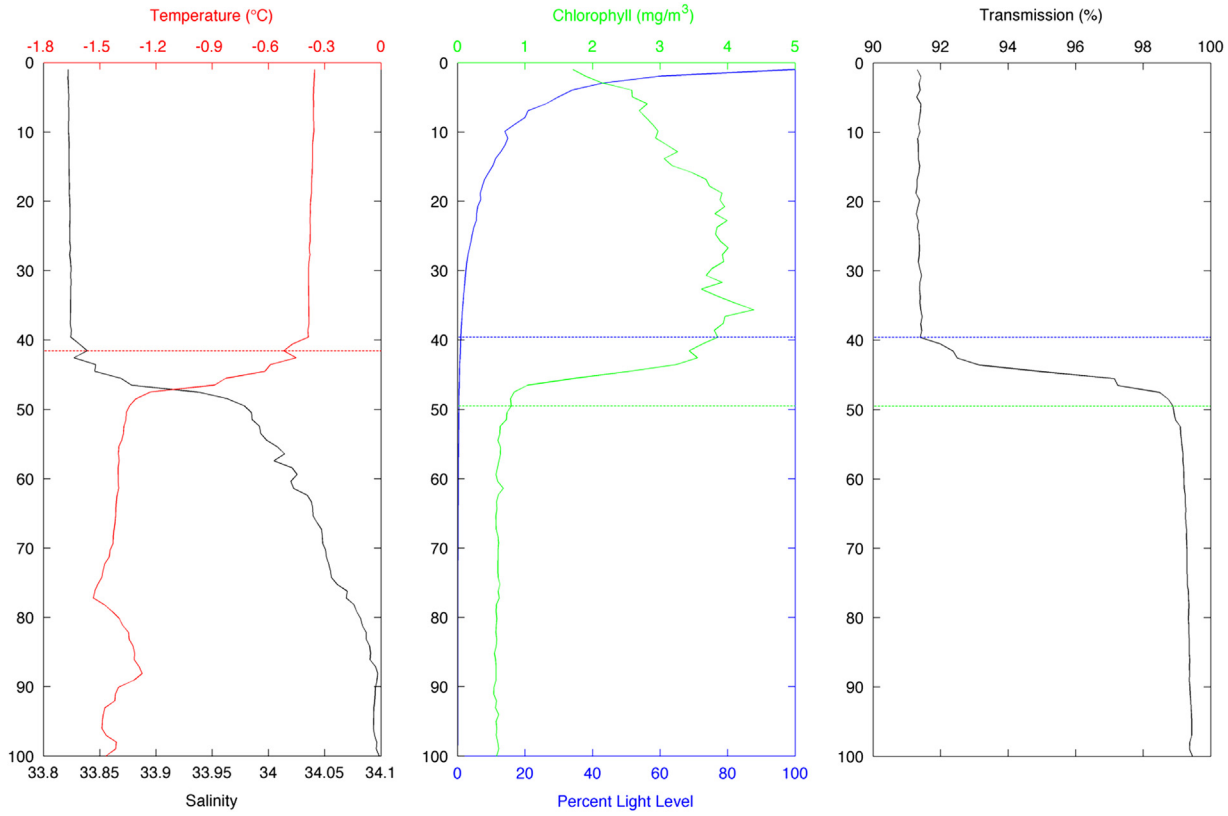

Fig. 5. Upper water column profile from the West Antarctic Peninsula to demonstrate the suitablity of the PPZ definition. Shown on the left are temperature (red) and salinity (black) where the horizontal line marks the depth of the mixed layer. Shown in the middle are the fluorescence (green) and percent light level (in blue, from the PAR sensor); the 1% light level is denoted by the dashed blue line and the PPZ depth is in green. On the right is the light transmission profile, shown with the euphotic zone and PPZ depths. (For interpretation of the references to color in this figure legend, the reader is referred to the web version of this article.)

specific C/^{234}Th ratio was used because of the anomalous features at depth. For L2 Station 1, the site-specific C/^{234}Th ratio was also used because of the shallow PPZ depth, outside the bounds of the regression. Uncertainty on the carbon fluxes is propagated from the ^{234}Th flux calculations and the standard deviations on the mean C/^{234}Th ratios in each depth bin.

3.1.4. *Spatial trends in ^{234}Th and upper ocean export*

In this discussion of spatial trends, we have classified the sampling locations as Thomalla et al. (2006) did for the Atlantic Ocean: temperate (35°–50°N and 35°–50°S), oligotrophic (20°–35°N and 5°–35°S), upwelling (5°–20°N), and equatorial (5°N–5°S) (Fig. 1, Table 1). In the northern hemisphere, the largest ^{234}Th deficits were found in the temperate and upwelling regions while the smallest deficits were found throughout the oligotrophic region (Fig. 9). In the southern hemisphere, deficits were largest to the south in the temperate region and smallest through the oligotrophic region, though not as small as in the northern hemisphere. Another interesting feature of the southern hemisphere transect is that between 5 and 25°S, the deficit of ^{234}Th extended deeper in the water column compared to stations to the north and south, perhaps due to a widening of the depth range of the deep chlorophyll maximum in this region.

Integrating over the area of the PPZ for each profile of ^{234}Th resulted in fluxes of ^{234}Th ranging from near zero at oligotrophic stations in the North Atlantic to 1848 dpm m^{-2} d^{-1} at 40°S in the temperate South Atlantic (Table 2, Fig. 10A). The mean flux of ^{234}Th in the oligotrophic regions of the North Atlantic was 307 ± 281 dpm m^{-2} d^{-1} (−275–805 dpm m^{-2} d^{-1}), three times lower than the mean flux across the oligotrophic region in the South Atlantic (1106 ± 334 dpm m^{-2} d^{-1}; 533–1709 dpm m^{-2} d^{-1}). Another key difference in ^{234}Th fluxes occurred from L1 to L2 in the eastern section of the North Atlantic; on L1, there was a decreasing offshore trend of ^{234}Th flux, with the lowest flux occurring at the TENATSO site (L1 Station 12). In contrast, when the same site was reoccupied the following year, the ^{234}Th flux was 6 times higher (L2 Station 24) and the second highest flux value measured in the North Atlantic during this study. One possible cause for this could be a difference in the atmospheric delivery of trace nutrients to the surface ocean in the two years, which could be corroborated with aerosol data once available.

Carbon fluxes were derived from ^{234}Th fluxes using the depth of the PPZ at each station and the regression of C/^{234}Th versus depth described above (Fig. 10B). The spatial trends observed in the ^{234}Th flux data are preserved in the carbon flux data, likely because of the small difference in C/^{234}Th ratios, driven by the small difference in C/^{234}Th ratios across the range of PPZ depths. The larger error bars on some of the carbon flux values are due to higher uncertainty on C/^{234}Th ratios when the PPZ was relatively shallow. The reasons for some of the geographic trends in ^{234}Th and carbon export become apparent when the fluxes are compared to monthly composite chlorophyll concentrations obtained from NASA's MODIS (Monthly, 4 km level 3 mapped, http://oceancolor.gsfc.nasa.gov/; Fig. 11). Chlorophyll concentrations were highest near the margins and in the temperate South Atlantic and corresponded with the highest values of export. The surface chlorophyll concentrations may crudely explain the difference in export from the oligotrophic regions in the North and South Atlantic; in the South Atlantic, surface chlorophyll is approximately four times higher compared to the North Atlantic. Finally, surface chlorophyll near the TENATSO site during L2 appeared to be approximately double that observed during L1.

The results from this study can be compared to previous studies in the same area (Fig. 12); however the methodological differences between the studies, such as integration depth and particle collection methods, may bias these comparisons (Charette and Moran, 1999; Santschi et al., 1999; Charette et al., 2001; Thomalla et al.,

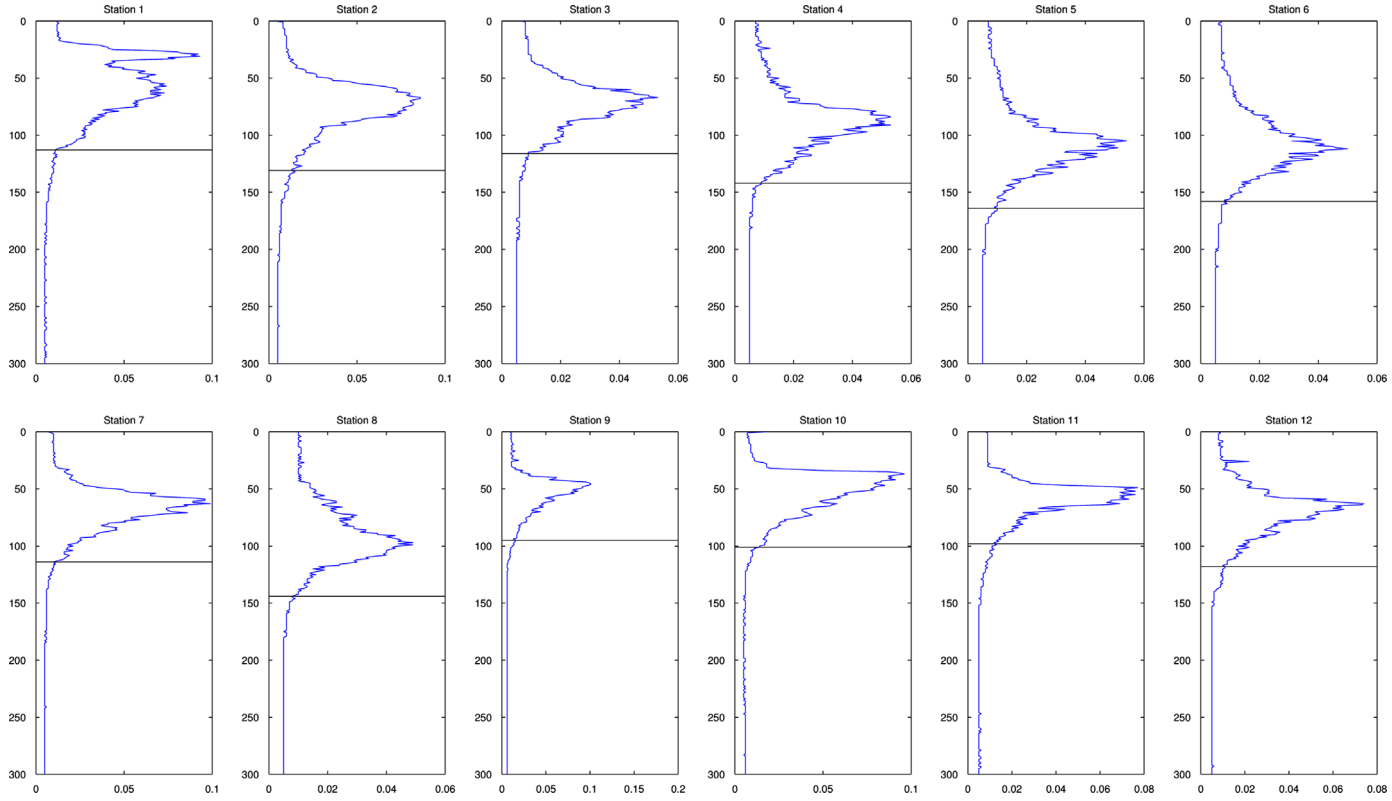

Fig. 6. Sample calculations of PPZ depths based on fluorescence profiles (depth versus volts), shown here in blue from U.S. GEOTRACES Leg 1. The PPZ depth is denoted by the black line. (For interpretation of the references to color in this figure legend, the reader is referred to the web version of this article.)

Table 1
Results from three GEOTRACES cruises in the Atlantic basin. ^{234}Th deficits were integrated to the depth of the primary production zone (PPZ). Carbon fluxes at each site were estimated using C/^{234}Th ratios based on a power law regression of C/^{234}Th ratios versus depth across all >51 μm C/^{234}Th data. Stations are classified as temperate (T), oligotrophic (O), upwelling (U), or equatorial (E).

	St	Lat	Long	Reg	^{234}Th flux $_{100\ m}$ (dpm m^{-2} d^{-1})	PPZ (m)	^{234}Th flux $_{PPZ}$ (dpm m^{-2} d^{-1})	C/Th $_{PPZ}$ (μmol dpm^{-1})	C flux $_{PPZ}$ (mmol m^{-2} d^{-1})
US 1	1	38.3	−9.7	T	687 ± 104	113	1041 ± 107	4.1	4.2 ± 0.4
US 1	2	36.8	−12.8	T	899 ± 141	131	928 ± 170	2.8	2.6 ± 0.8
US 1	3	35.2	−16.0	T	295 ± 100	116	326 ± 107	3.1	1.0 ± 0.5
US 1	4	33.1	−19.0	O	412 ± 106	142	534 ± 151	2.6	1.4 ± 0.5
US 1	5	31.0	−22.0	O	334 ± 131	164	472 ± 165	2.3	1.1 ± 0.5
US 1	6	27.5	−22.0	O	−229 ± 116	158	−227 ± 134	2.4	−0.5 ± 0.4
US 1	7	24.0	−22.0	O	557 ± 88	114	623 ± 98	3.1	2.0 ± 0.7
US 1	8	21.0	−22.0	O	743 ± 107	144	805 ± 130	2.6	2.1 ± 0.7
US 1	9	17.4	−18.3	U	1084 ± 96	95	1150 ± 91	3.6	4.2 ± 1.8
US 1	10	17.4	−20.8	U	720 ± 99	101	820 ± 96	3.5	2.8 ± 1.3
US 1	11	17.4	−22.8	U	658 ± 87	98	741 ± 85	3.5	2.6 ± 1.2
US 1	12	17.4	−24.5	U	68 ± 84	118	186 ± 94	3.0	0.6 ± 0.3
US 2	1	39.7	−69.8	T	1372 ± 123	54	801 ± 68	6.7	5.3 ± 0.4
US 2	2	39.4	−69.5	T	1576 ± 96	73	1436 ± 60	4.5	6.4 ± 2.9
US 2	3	38.7	−69.1	T	1277 ± 100	87	554 ± 80	3.9	2.2 ± 1.1
US 2	4	38.3	−68.9	T	549 ± 107	157	148 ± 113	2.4	0.4 ± 0.3
US 2	5	38.1	−68.7	T	998 ± 126	156	499 ± 136	2.4	1.2 ± 0.5
US 2	6	37.5	−68.4	T	927 ± 103	106	835 ± 89	3.3	2.8 ± 1.3
US 2	8	35.4	−66.7	T	680 ± 110	117	286 ± 97	3.1	0.9 ± 0.4
US 2	10	31.7	−64.2	O	377 ± 133	197	−275 ± 159	2.0	−0.6 ± 0.3
US 2	11	30.8	−60.8	O	862 ± 146	155	480 ± 160	2.5	1.2 ± 0.5
US 2	12	29.7	−56.8	O	1007 ± 120	184	495 ± 158	2.1	1.1 ± 0.5
US 2	13	28.6	−53.2	O	544 ± 151	182	449 ± 185	2.2	1.0 ± 0.5
US 2	14	27.6	−49.6	O	831 ± 108	181	148 ± 138	2.2	0.3 ± 0.3
US 2	15	26.9	−47.2	O	688 ± 156	191	421 ± 199	2.1	0.9 ± 0.4
US 2	16	26.1	−44.8	O	444 ± 130	185	66 ± 154	2.1	0.1 ± 0.3
US 2	17	25.1	−42.5	O	662 ± 161	186	206 ± 197	2.1	0.4 ± 0.4
US 2	18	24.2	−40.2	O	448 ± 120	193	181 ± 153	2.1	0.4 ± 0.3
US 2	19	23.3	−38.1	O	350 ± 154	172	251 ± 168	2.3	0.6 ± 0.4
US 2	20	22.3	−35.9	O	372 ± 132	174	266 ± 146	2.2	0.6 ± 0.4
US 2	21	20.9	−32.6	O	501 ± 141	126	318 ± 151	2.9	0.9 ± 0.5
US 2	22	19.4	−29.4	U	281 ± 135	139	−14 ± 141	2.7	0.0 ± 0.4
US 2	23	18.4	−26.8	U	1240 ± 142	140	604 ± 221	2.7	1.6 ± 0.7
US 2	24	17.4	−24.5	U	723 ± 137	111	1088 ± 138	3.2	3.5 ± 1.2
DT	1	−49.6	−52.7	T	1519 ± 66	99	1503 ± 65	3.5	5.3 ± 2.3
DT	2	−49.0	−48.9	T	1859 ± 66	94	1848 ± 63	3.6	6.7 ± 2.8
DT	3	−46.9	−47.2	T	962 ± 66	89	1077 ± 61	3.8	4.1 ± 2.2
DT	4	−44.7	−45.6	T	1264 ± 66	86	1227 ± 59	3.9	4.8 ± 2.5
DT	5	−42.4	−44.0	T	1786 ± 77	69	1679 ± 61	4.6	7.8 ± 3.4
DT	6	−40.0	−42.5	T	1771 ± 66	88	1655 ± 60	3.8	6.4 ± 3.3
DT	7	−37.8	−41.1	T	1335 ± 66	153	1317 ± 93	2.5	3.3 ± 1.0
DT	8	−35.0	−39.4	T	708 ± 66	149	882 ± 90	2.5	2.2 ± 0.7
DT	9	−32.1	−37.5	O	841 ± 66	160	922 ± 96	2.4	2.2 ± 0.7
DT	10	−29.1	−35.8	O	631 ± 67	146	533 ± 89	2.6	1.4 ± 0.4
DT	11	−26.1	−34.3	O	1010 ± 66	168	1075 ± 100	2.3	2.5 ± 0.8
DT	12	−22.5	−32.7	O	794 ± 66	188	1018 ± 108	2.1	2.1 ± 0.7
DT	13	−17.0	−30.6	O	987 ± 66	194	1267 ± 111	2.1	2.6 ± 0.6
DT	14	−12.9	−29.2	O	870 ± 66	231	1078 ± 126	1.8	1.9 ± 0.6
DT	15	−9.2	−28.0	O	1018 ± 65	197	1709 ± 113	2.0	3.5 ± 0.7
DT	16	−5.7	−28.5	O	866 ± 67	163	1242 ± 96	2.4	2.9 ± 0.9
DT	17	−2.6	−28.9	E	1686 ± 67	119	1723 ± 76	3.0	5.2 ± 1.7
DT	18	−0.2	−32.9	E	1218 ± 66	137	1218 ± 85	2.7	3.3 ± 0.9

2006; Buesseler et al., 2008a). These five studies used variable integration depths of 100 m (Charette and Moran, 1999; Santschi et al., 1999; Charette et al., 2001), 150 m (Buesseler et al., 2008a), and the ^{234}Th–^{238}U equilibrium depth (Thomalla et al., 2006) to calculate ^{234}Th and carbon fluxes. Again, this difference in depth affects both the depth range over which the flux is derived and the C/^{234}Th value that is used. Similarly, the studies used different methods of collecting sinking or large particles including collection of >51 μm particles with in situ pumps (Charette et al., 2001; Thomalla et al., 2006; Buesseler et al., 2008a) or pumping from a rosette (Charette and Moran, 1999) or from sediment traps (Santschi et al., 1999). Each C/^{234}Th method is potentially susceptible to its own biases (Buesseler et al., 2006) such as artificially high particulate carbon or adsorption of dissolved organic carbon during filtration that could lead to too high C/^{234}Th ratios when particles are sampled from bottles (Moran et al., 1999). *In situ* pumps may break up carbon rich particles due to the high pressure differentials across the filter and thus result in artificially low C/^{234}Th ratios (Gardner et al., 2003). Finally, some sediment traps are subject to a host of biases that may positively or negatively bias C/^{234}Th ratios including in-trap sample dissolution, hydrodynamic biasing, and possible inclusion of C rich swimmers (Buesseler et al., 2006). One analytical concern when measuring particulate ^{234}Th samples of variable composition and loading is self-absorption biases on beta detection efficiencies. Work carried out during the GEOTRACES intercalibration process suggested however that the detector efficiency did not change significantly for particles from different regions (Maiti et al., 2012). To minimize any detector biases due to particle loading on the filters, in this study, samples were split across multiple silver filters, when necessary, in very particle-rich regions. It is important to keep this host of methodological differences and sample variability in mind when comparing these different studies.

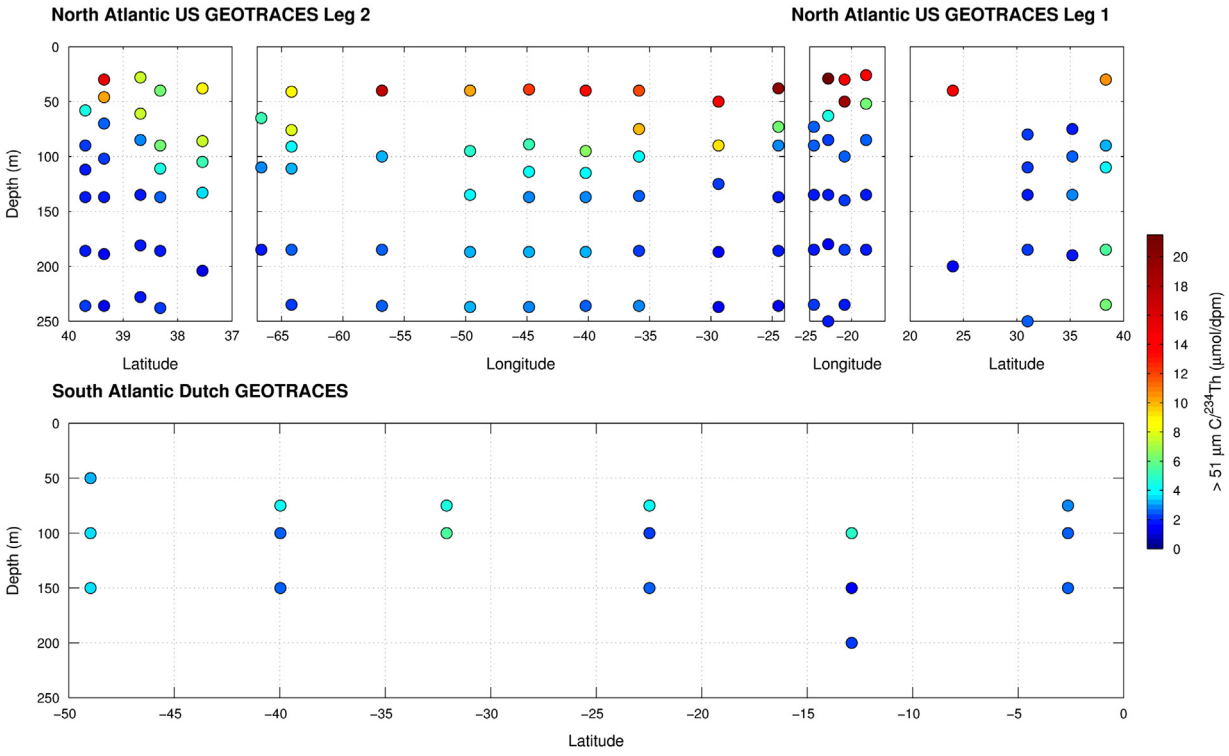

Fig. 7. C/^{234}Th geographic distribution in the North and South Atlantic.

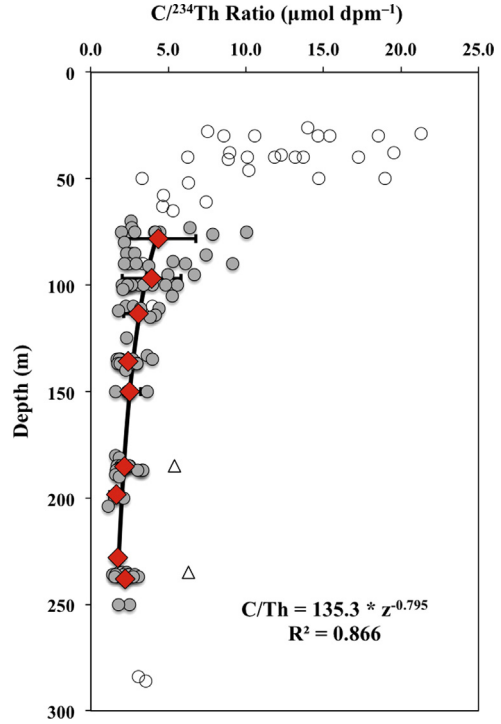

Fig. 8. C/^{234}Th ratios from large (> 51 µm) particles on all three cruises. A power law regression was derived within the depth ranges of calculated PPZs (values in grey), using 20 m-binned averages (red diamonds). This regression was used to calculate C/^{234}Th ratios at the PPZ depth of individual stations (Table 1). In white are values shallower and deeper than the range of PPZ depths. The data represented by the white triangles are from L1 Station 1 and were not included in the regression. (For interpretation of the references to color in this figure legend, the reader is referred to the web version of this article.)

Prior measurements in the temperate North Atlantic were all significantly higher than those measured here when compared both at the PPZ and 100 m. This difference is driven largely by two

Table 2
Summary of carbon flux estimates in the regions shown in Fig. 1 from this study.

		This study		
		n	C flux at PPZ (mmol m^{-2} d^{-1})	C flux at 100 m (mmol m^{-2} d^{-1})
Temperate	35°–45°N	10	2.7 ± 2.0	3.0 ± 1.3
Oligotrophic	20°–35°N	17	0.8 ± 0.7	1.8 ± 1.0
Upwelling	5°–20°N	7	2.2 ± 1.5	2.4 ± 1.4
Equatorial	5°S–5°N	2	4.3 ± 1.4	5.1 ± 1.2
Oligotrophic	5°–35°S	8	2.4 ± 0.6	3.0 ± 0.4
Temperate	35°–50°S	8	5.1 ± 1.9	4.9 ± 1.5

measurements, the first in the western part of the basin, where high carbon flux was measured on the Scotian shelf, in association with a region of increased primary productivity (Charette et al., 2001). Similarly, in the eastern basin, Thomalla et al. (2006) measured high export flux following a period of increased productivity, hypothesized to have been triggered by nutrient injection from depth. Both of those measurements fall within the upper range measured during the North Atlantic Bloom Experiment (NABE), where POC flux from the euphotic zone ranged from 5 to 41 mmol m^{-2} d^{-1} (Buesseler et al., 1992), whereas the new data presented here fall to the lower end or below the range of fluxes observed during NABE. In the temperate region of the South Atlantic, there was only one prior measurement by Thomalla et al. (2006) which did not differ significantly from our measurements.

In this and prior studies, carbon export in the oligotrophic regions is very low and highly variable, ranging from 0 mmol m^{-2} d^{-1} up to 12 mmol m^{-2} d^{-1}. During this study, zero or near zero fluxes were measured on several occasions in the

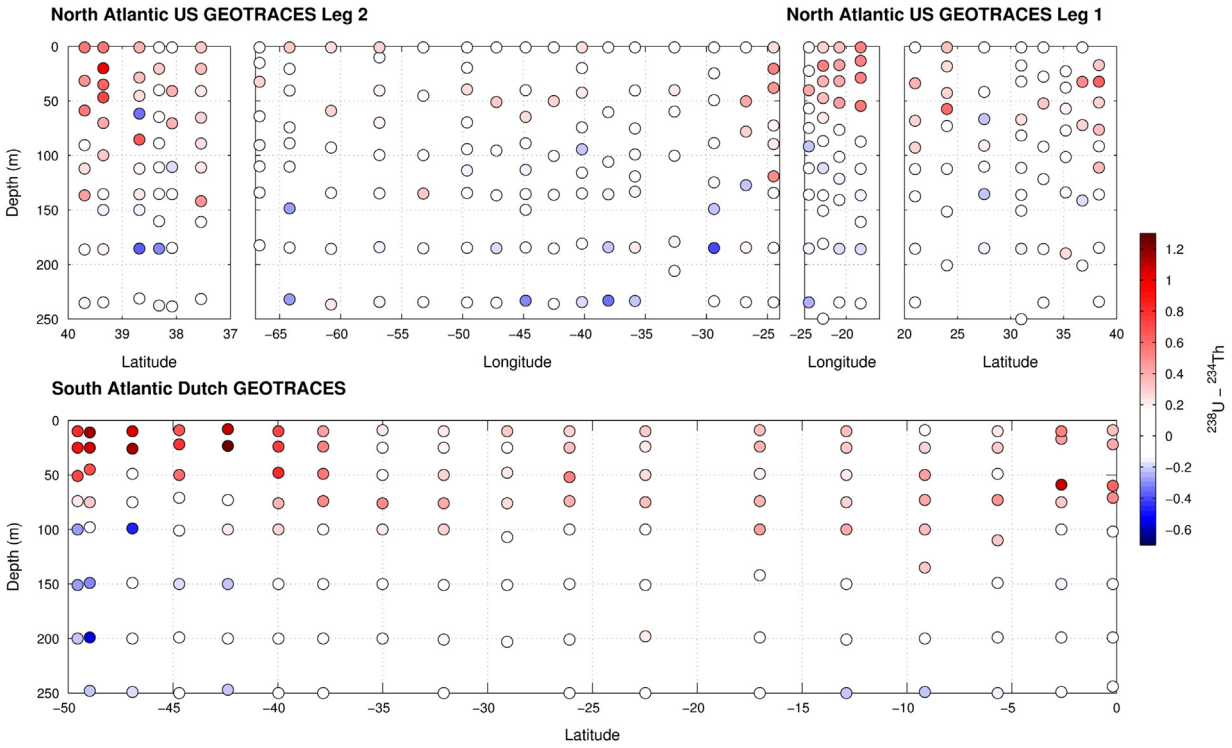

Fig. 9. Summary of ^{234}Th deficits (^{238}U minus ^{234}Th) in the upper water column along three GEOTRACES transects. Red shades indicate areas of deficit, blue shades show areas of excess, and white values are where ^{234}Th and ^{238}U are within the analytical uncertainty of secular equilibrium.

oligotrophic regions, as previously measured by Thomalla et al. (2006) during a non-bloom period in the northern subtropical gyre. In both this and prior studies, the oligotrophic fluxes in the Southern Atlantic were higher than those in the North Atlantic, potentially driven by the passage of eddies, which have sometimes been shown to have a dramatic impact on biogeochemistry in oligotrophic regions. For example, in the subtropical North Atlantic, Sweeney et al. (2003) noted that upwelling eddies were associated with four out of six instances where ^{234}Th fluxes exceeded 1000 dpm m^{-2} d^{-1}. While oligotrophic fluxes in the North Atlantic never exceeded this value during this study, the mean flux of ^{234}Th in the oligotrophic South Atlantic was higher, at 1106 ± 334 dpm m^{-2} d^{-1}.

Carbon fluxes were most different in the equatorial and upwelling regions, likely due to differences in primary productivity drivers. Charette and Moran (1999) were able to attribute their large flux measurements in these regions in May 1996 to increased dust input, though it is possible, as discussed above that some of this difference is due to high C/^{234}Th measurements from the rosette collection method. These flux differences highlight the importance of measuring both surface and atmospheric species in the GEOTRACES program in order to understand fluxes and species distributions. The largest difference between these measurements of ^{234}Th and those reported in prior studies is significant depth and spatial coverage achieved by the GEOTRACES program. The flux measurements presented here are a significant contribution to the existing set of data and will provide a larger framework on which to parameterize particle fluxes in global biogeochemical models.

3.1.5. *Subsurface remineralization*

Excesses of ^{234}Th immediately below the surface deficit have been reported in prior studies (Savoye et al., 2004; Buesseler et al., 2008a; Maiti et al., 2010; Planchon et al., 2012) and are indicative of particle remineralization by heterotrophic bacteria and zooplankton. Higher resolution sampling made possible by small-volume ^{234}Th methods has allowed for the elucidation of these features. The short half-life of ^{234}Th implies that this remineralization has happened within days to several weeks of sampling. In the ^{234}Th profiles from the North Atlantic, examples of these excesses are evident throughout the temperate, oligotrophic, and upwelling regions (Figs. 2 and 3). In most cases, these excesses are small deviations from equilibrium, regardless of the size of the deficit above. Significant deviations from equilibrium ($>10\%$) were observed at L1 Station 12 and L2 Stations 3, 4, 6, 8, 10, 16, 19, and 22, even though ^{234}Th fluxes were indistinguishable from zero at some of these stations. The presence of these remineralization features at these extremely low flux stations combined with the short half-life of ^{234}Th could be indicative of episodic export events where the flux signal has occurred previously, but remineralization is still occurring. During the EDDIES program, only by combining profiles taken at high spatial resolution were similar remineralization features observable (Buesseler et al., 2008a); in many studies due to limited horizontal and sub-euphotic zone vertical resolution, these features are only defined by a single data point. Another possibility is that these features have been advected from regions of high export and thus higher remineralization as has been suggested in prior studies (Cai et al., 2008).

3.2. *^{234}Th in intermediate and deep waters*

There has only been limited sampling of ^{234}Th in the intermediate water column because of its primary application in the upper water column. It has been used however to examine near-bottom particle dynamics including sediment resuspension and scavenging by hydrothermal plumes. This new data set, primarily from the U.S. GEOTRACES cruises, is the most extensive survey of ^{234}Th below 1000 m. Below the depths of intense particle production, export, and remineralization in the surface and removed from

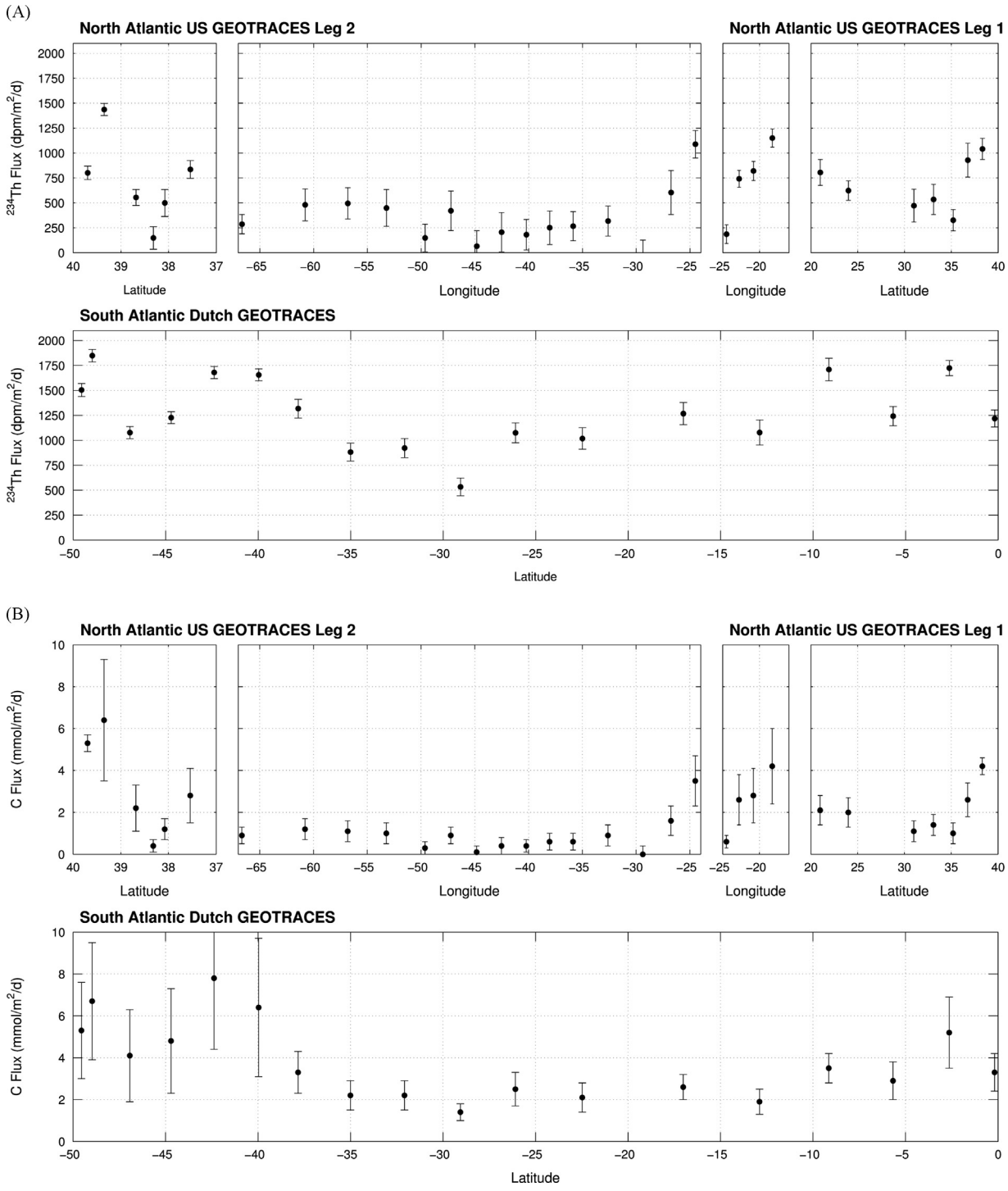

Fig. 10. (A) ^{234}Th fluxes at the PPZ depth in the North and South Atlantic. (B) Carbon fluxes estimated from ^{234}Th fluxes and C/^{234}Th ratios at the PPZ depth.

resuspension processes near the bottom and margins, ^{234}Th and ^{238}U are expected to be in equilibrium. As these new data reveal, this may not always be the case.

3.2.1. *^{234}Th in Mediterranean Outflow Water*

Mediterranean Outflow Water (MOW) spills out of the Mediterranean Sea through the Strait of Gibraltar into the Gulf of Cadiz and the Eastern Atlantic Ocean (Ambar et al., 2002). This warm, saline water mass is often evident between depths of 800 to 1200 m. The MOW also carries with it a plume of suspended particulate matter from its interaction with the seafloor in the Strait and the Gulf of Cadiz. In this study, L1 stations 1 to 6 were located within the region where eddies formed from MOW have been know to propagate eastward, however only at station 1 is the influence of MOW on ^{234}Th apparent (Fig. 13). The MOW at this station ranged from 500 to 1500 m and coincided with a 10% deficit of total ^{234}Th relative to ^{238}U. Large particles were only measured in the upper 1000 m, but at this depth, there was approximately a four-fold increase in >51 μm ^{234}Th. In the smaller size class, particulate ^{234}Th was elevated over the same depth range and was higher than even surface values. Both the increase in particulate ^{234}Th and deficit in total ^{234}Th imply recent scavenging of ^{234}Th onto particles and subsequent removal to

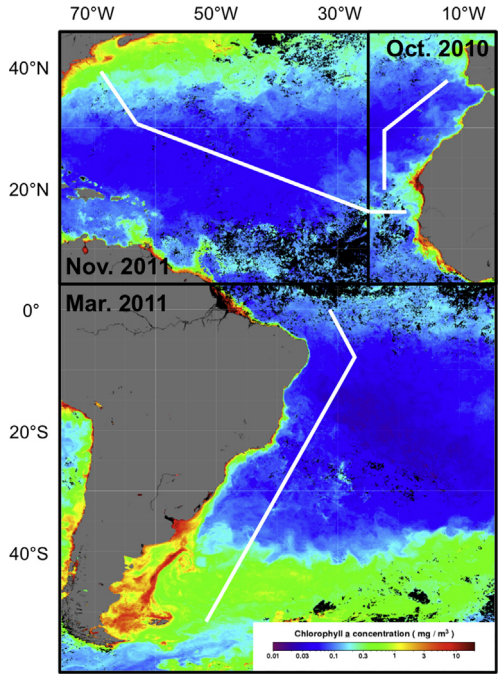

Fig. 11. Monthly composites of surface chlorophyll from MODIS for each cruise. The TENATSO site is located at 17.4°N × 24.5°W. (For interpretation of the references to color in this figure legend, the reader is referred to the web version of this article.)

deeper in the water column, similar to previous observations by Schmidt (2006).

3.2.2. ^{234}Th in the TAG hydrothermal plume

Neutrally buoyant plumes can emanate from hydrothermal systems and extend up to tens or hundreds of kilometers from their source. Iron and manganese rich particles in these plumes can scavenge reactive species from the water column like ^{234}Th (Kadko, 1996) which can subsequently be used to determine scavenging rates onto particles and removal rates to the seafloor. This technique has been demonstrated using ^{234}Th at venting sites on the Juan de Fuca ridge in the Pacific (Kadko et al., 1994) and at the TAG hydrothermal site in the Atlantic (German et al., 1991).

The TAG hydrothermal field was sampled at Station 16 on L2 and identified based on transmissometry (Fig. 14). The depth of the plume can vary on relative short time scales; on the down-cast of the *in situ* pumps, the maximum beam attenuation coefficient value was at 3318 m whereas on the up-cast the maximum was at 3186 m. Previous observations of the plume placed it between 3300 and 3500 m (German et al., 1991). Through the plume, there was little disequilibrium between total ^{234}Th and ^{238}U, only a 7 to 10% excess. However, there was a large deficit of dissolved ^{234}Th (total minus particulate) relative to ^{238}U at 3300 m. At this depth, 50% of the total ^{234}Th was particulate, which was significantly different from conditions above and below the plume (>95% dissolved ^{234}Th) and consistent with measurements from TAG and other hydrothermal plumes (German et al., 1991; Kadko et al., 1994).

With the dissolved and particulate ^{234}Th data, we can calculate the net rate of scavenging of ^{234}Th (J_{Th}) onto particles in the plume. The equation to express the rate of change in dissolved ^{234}Th with respect to time is:

$$\frac{\partial^{234}\mathrm{Th}_d}{\partial t} = \left(^{238}\mathrm{U} - ^{234}\mathrm{Th}_d\right)\lambda - J_{Th}$$

$^{234}\mathrm{Th}_d$ and ^{238}U are the activities of the dissolved species integrated over the depth of the plume and λ is the decay constant of ^{234}Th. In the above formulation, physical transport processes are neglected as there are neither measurements of near-bottom transport at this site yet available nor were we able to estimate a thorium gradient as we only identified the hydrothermal signal at this single station. Assuming steady state, the net rate of ^{234}Th scavenging onto particles is:

$$J_{Th} = (^{238}\mathrm{U} - ^{234}\mathrm{Th}_d)\lambda$$

The mean lifetime of dissolved ^{234}Th with respect to removal onto particles (τ_d) is:

$$\tau_d = \frac{^{234}\mathrm{Th}_d}{J_{Th}}$$

Integrating over the deficit of dissolved ^{234}Th, from 3000 to 3505, the net scavenging rate was 0.91 dpm cm^{-2} d^{-1} and the mean lifetime of dissolved ^{234}Th in the plume was 100 days. Where the dissolved ^{234}Th was lowest, the mean life of ^{234}Th was as only 33 days. These values are of a similar order of magnitude as those measured on the Juan de Fuca ridge (Kadko et al., 1994). In comparison, between 1500 and 2100 m at this station, the mean lifetime of dissolved ^{234}Th is greater than six times its half-life. While ^{234}Th was effectively scavenged in the plume, the lack of a deficit in total ^{234}Th indicates that the particles were slow sinking and there was no removal occurring on the time-scales observable with ^{234}Th.

3.2.3. ^{234}Th disequilibria at intermediate depths

Disequilibria of ^{234}Th at intermediate depths (>500 m to 1000 m off the bottom) have been identified in only a few studies and often defined by only one or two data points. One case, as described above, was caused by the influence of Mediterranean Outflow Water (Schmidt, 2006). Other instances however have been identified further away from ocean margins in the subtropical Atlantic (Owens et al., 2011) and Pacific (Benitez-Nelson et al., 2001a), the Southern Ocean (Coppola et al., 2005), and the Gulf of Mexico (Baskaran et al., 1996).

On the GEOTRACES transects in the North Atlantic, mid-water column deficits were observed at Stations 7 and 12 on L1 (Fig. 15) and Stations 12, 18, and 24 on L2 (Fig. 16). In two of these cases, the deficits were only measured at a single depth (L1 St. 12 and L2 St. 18), but in the other three cases, the deficits spanned widely spaced samples over a range of up to 3500 m. In all cases, the deviation from equilibrium ranged from 4 to 9%, beyond the range of uncertainty for our measurements of ^{234}Th and ^{238}U, and there was no change in the partitioning of total ^{234}Th between the dissolved and particulate phases. That these features are visible in ^{234}Th data suggests that whatever process created them occurred within days or weeks of our measurements. At the two stations in the center of the gyre, it is unlikely that these features were due to seafloor interactions and are more likely due to a local process. In the previous observation of these features in the subtropical Atlantic, one instance was caused by low ^{238}U concentrations, but in the second case, the feature was unique to ^{234}Th (Owens et al., 2011). A local process that transforms suspended particles into sinking particles, such as fecal pellet production (Sutherland et al., 2010) or accumulation and aggregation at density gradients (MacIntyre et al., 1995), could possibly create deficits in ^{234}Th at these depths. The other stations where deficits were observed at depth were closer to the ocean margin in the Eastern Atlantic, so it is possible that these features may be due to interaction with continental shelf material and lateral transport. Measurements of radium isotopes and particle composition may be helpful in determining the source of these deficit signals. It might also be worthwhile to analyze ^{238}U samples from some of these stations to confirm that the changes occur in ^{234}Th rather its parent isotope (Owens et al., 2011).

At many stations in the North Atlantic, excesses were observed well below the PPZ (L1: St. 3, 9, 10, 11, 12, Fig. 15; L2: 2, 6, 8, 14, 20, 22, Fig. 16) and varied from equilibrium by 4 to 12%. The cause of these

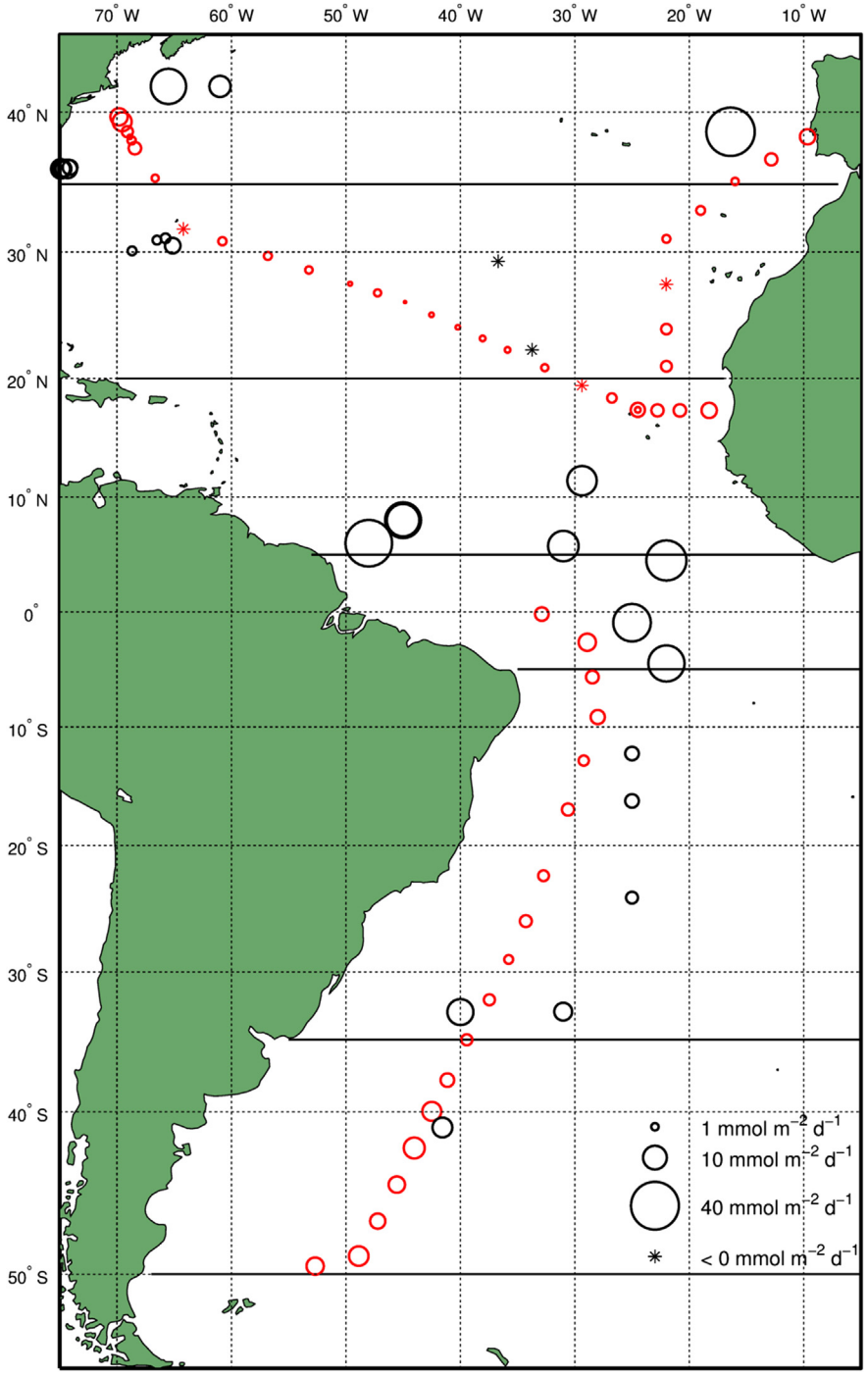

Fig. 12. Comparison of POC fluxes from this study (in red) to other ^{234}Th-derived estimates of POC export (in black). Note, these studies used different integration depths of 100 m (Charette and Moran, 1999; Santschi et al., 1999; Charette et al., 2001), 150 m (Buesseler et al., 2008a), and the ^{234}Th-^{238}U equilibrium depth (Thomalla et al., 2006) to calculate ^{234}Th and carbon fluxes.

excesses that span hundreds to thousands of meters is not apparent from these data alone as there was no significant change in partitioning of ^{234}Th between dissolved and particulate phases or changes in the beam attenuation coefficient at these depths. Where possible, we will compare these data to ^{228}Th ($t_{1/2}$ = 1.9 y), which may be able to provide more information about the lifespan of these features or whether they are artifacts of our analytical technique.

These deficit and excess features through the mid-water column pose some methodological quandaries such as how the mid-water ratio of ^{234}Th to ^{238}U is used to determine beta counter efficiency and how ^{234}Th fluxes are modeled in the water column. As described in Section 2.2.3, the detectors' efficiency was determined by adjusting their efficiency to minimize the percent difference between mean values of ^{238}U and ^{234}Th taken from the mid-water column. Points that were significant deviations from equilibrium were deliberately removed to avoid interfering with this calibration. In other studies however, where sampling below the euphotic zone may be very limited, if excess or deficit features were present, this could bias an entire data set positively or negatively. Another issue that these features raise relates to how ^{234}Th fluxes are modeled and calculated. In a 1-D model steady-state model, excesses and deficits over the full water column would be expected to balance one another out. While not surprising, these features demonstrate that 1-D flux models, as presented here, are not the best descriptor of particle flux and transport in the ocean. As

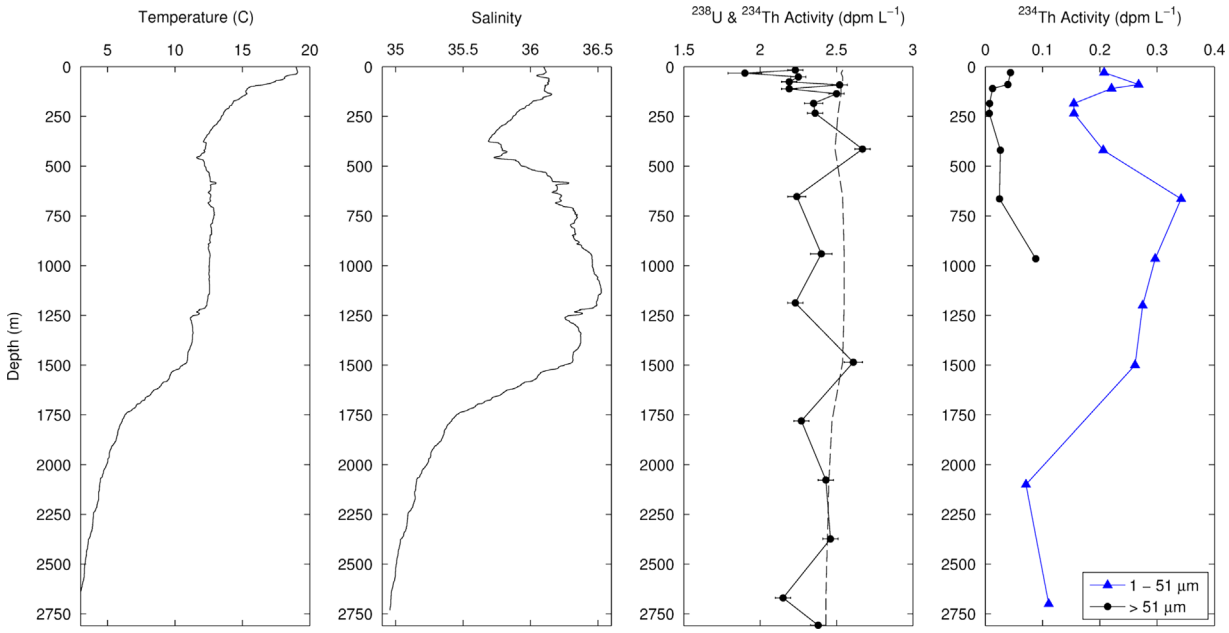

Fig. 13. Hydrographic and ^{234}Th data from L1 Station 1, where the influence of Mediterranean Outflow Water on total and particulate ^{234}Th is visible between 500 and 1500 m.

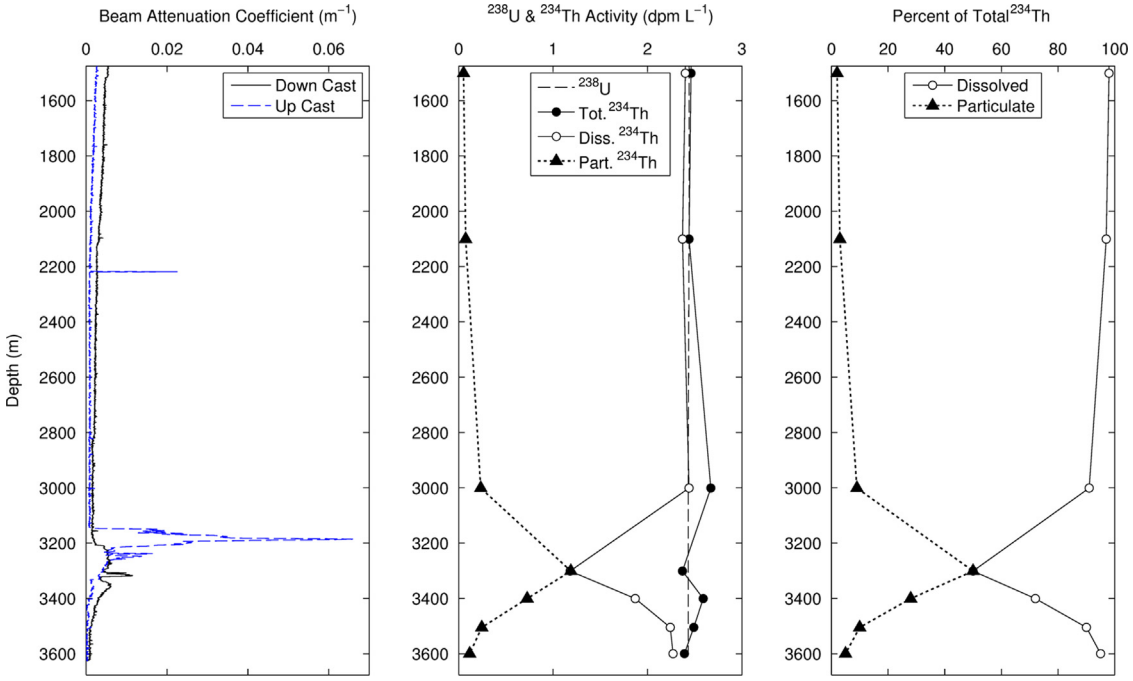

Fig. 14. Beam attenuation coefficient (derived from transmission measured by the CTD below the *in situ* pumps) near the TAG hydrothermal plume (left). The effect of the hydrothermal plume on activity and partitioning of ^{234}Th (center and right).

larger data sets like this begin to reveal these features, it is important that we take these observations and use them to improve our methods and analyses in the future.

3.2.4. *^{234}Th in benthic nepheloid layers*

While few measurements of ^{234}Th have been made in the mid-water column, ^{234}Th has been more widely applied to understand particle dynamics near the seafloor in benthic nepheloid layers (BNL). Nepheloid layer scavenging of ^{234}Th typically manifests itself as an increase in particulate ^{234}Th and a decrease in dissolved and total ^{234}Th, implying scavenging onto particles and resettling to the seafloor (Bacon and Rutgers van der Loeff, 1989; Turnewitsch and Springer, 2001; Rutgers van der Loeff et al., 2002; Inthorn et al., 2006; Turnewitsch et al., 2008).

Large BNL were observed at Stations 4 through 10 in the western North Atlantic (Fig. 16), but the full water column was only sampled at Stations 8 and 10 due to high current speeds resulting in a large wire angle during deployments at Stations 4 and 6. At Station 8, particulate ^{234}Th increased towards the bottom, total ^{234}Th was in equilibrium, and dissolved ^{234}Th decreased. The deficit of dissolved ^{234}Th is indicative of scavenging of ^{234}Th onto particles but the equilibrium of total ^{234}Th with ^{238}U suggests that settling rates out of the BNL are slow. The BNL at

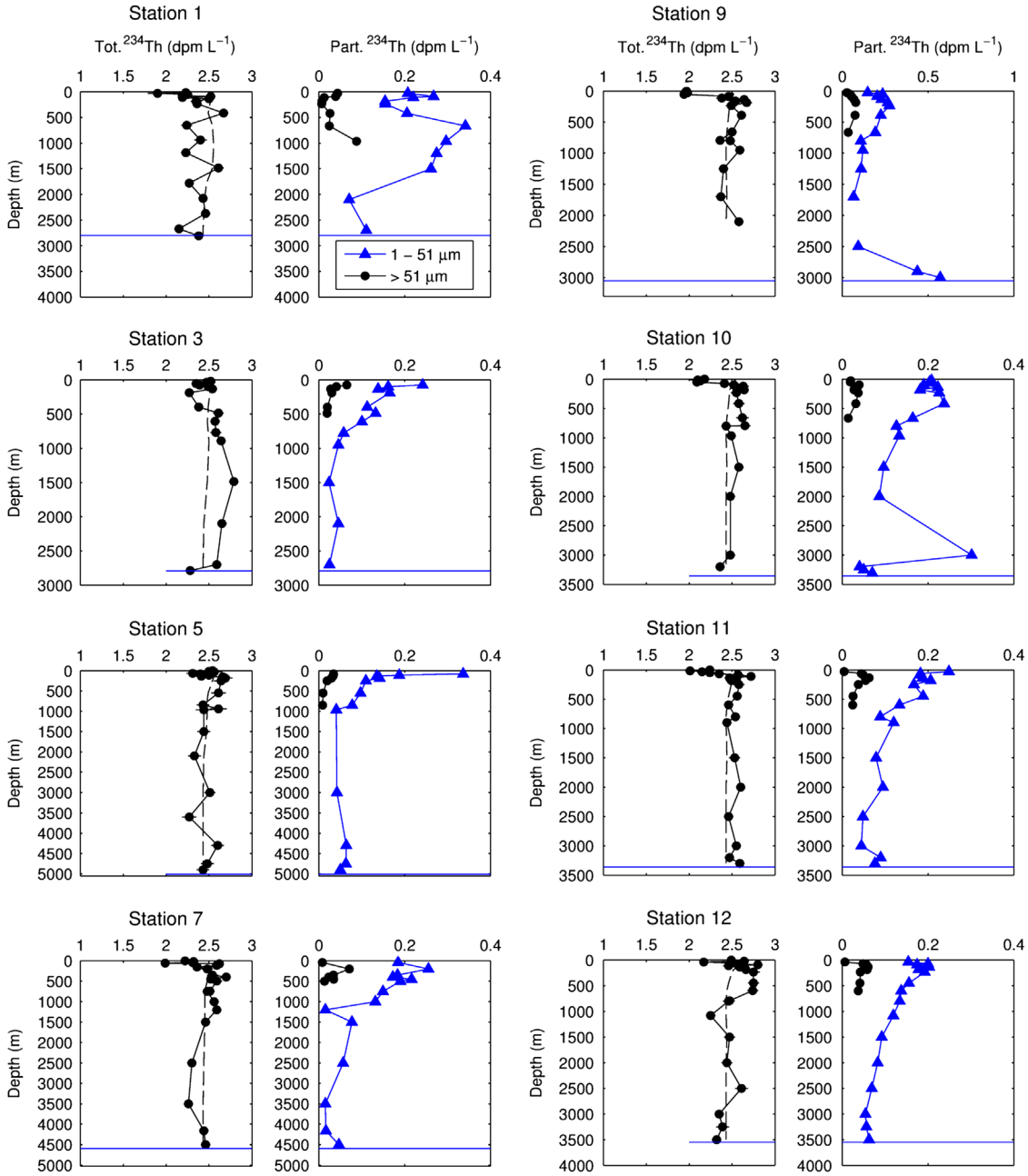

Fig. 15. Full profiles of total and particulate ^{234}Th on L1. Bottom depth is denoted by the solid blue line. (For interpretation of the references to color in this figure legend, the reader is referred to the web version of this article.)

Station 10 spanned a larger depth range but was less intense compared to Station 8. There was an excess of total ^{234}Th in the upper part of the BNL, but ^{234}Th was in equilibrium near the bottom. At the bottom, there was a deficit of dissolved ^{234}Th due to the peak in particulate ^{234}Th. This deficit in dissolved ^{234}Th implies scavenging, but the unusual excess further above the seafloor might suggest some complex recycling of local or advected particulate material. Measurements of radium isotopes and longer-lived thorium isotopes will provide more information on mixing rates and scavenging near the seafloor.

4. Conclusions

With the two transects of ^{234}Th across the North and South Atlantic, the spatial information on particle export from this tracer has increased dramatically. Particle flux patterns, highest near the margins and lowest in the subtropical regions, were consistent with expectations and previous measurements. Particularly because of its large geographic scope, this data set was also useful for reiterating the importance of using a biologically meaningful depth rather than a fixed depth to calculate euphotic zone particle flux.

With the GEOTRACES program, changes in ^{234}Th with depth have also been better resolved than ever before. Of particular interest are the deficits and excesses through the mid-water column (1000 m to 1000 m above the bottom), where equilibrium between ^{234}Th and ^{238}U is expected. Although we cannot yet identify a cause for each of these features, their recurrence lends credence to prior observations of similar features. Analysis of archive ^{238}U samples at some of these stations may be worthwhile, to confirm that the observed features are due to ^{234}Th. Also, concurrent measurements of ^{228}Th may corroborate some evidence of these features.

When combined with measurements of metal to ^{234}Th ratios on particles, the fluxes derived here will be important for constraining

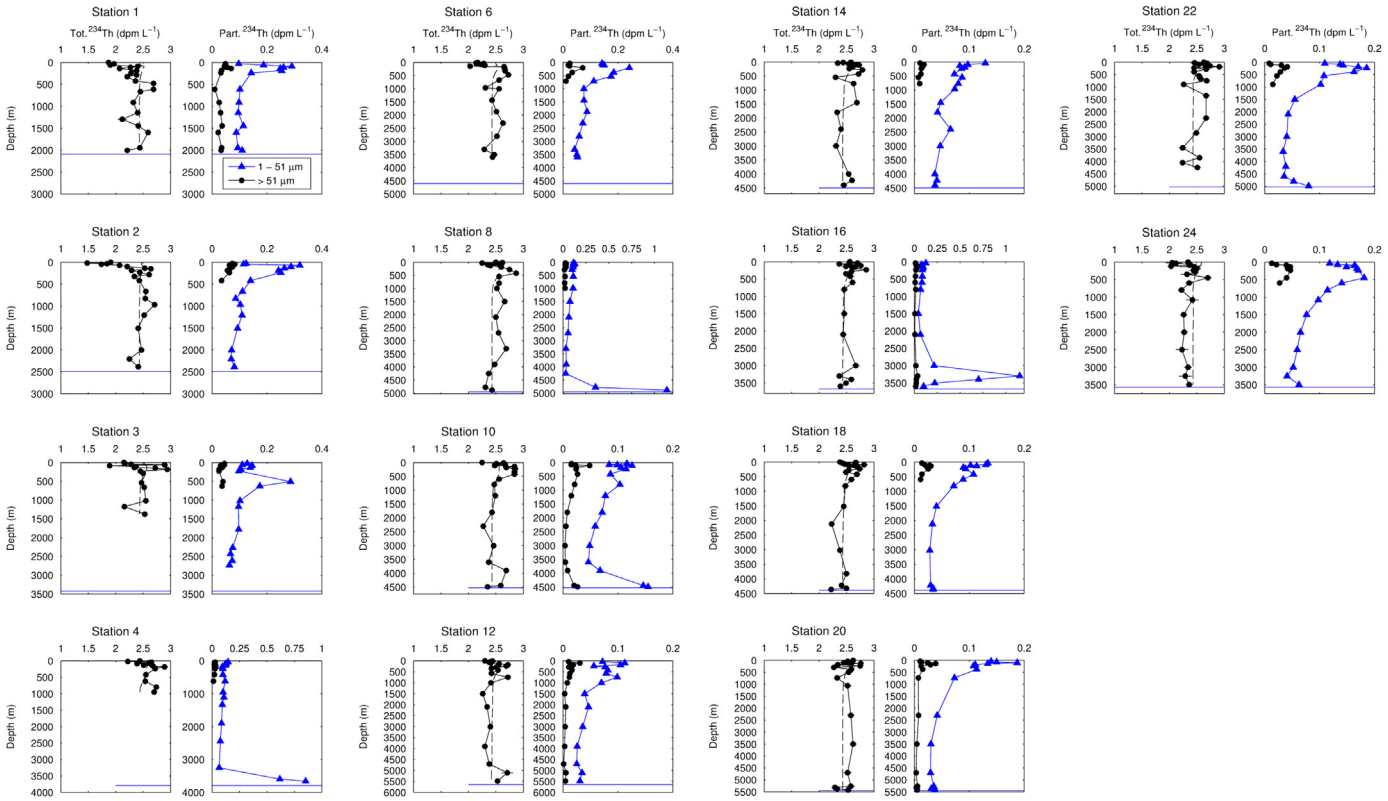

Fig. 16. Full water column profiles of total and particulate Th-234 on L2. Bottom depth is denoted by the solid blue line. (For interpretation of the references to color in this figure legend, the reader is referred to the web version of this article.)

budgets of trace metals measured by others in the GEOTRACES program. These data may also contribute to our understanding of particle cycling in the ocean. Marchal and Lam (2012) demonstrated that the GEOTRACES program is poised to improve estimates of rates of adsorption, desorption, remineralization and aggregation of small particles, and disaggregation and sinking of larger particles in the ocean by the modeling of multiple thorium isotopes with different half lives (^{234}Th, ^{228}Th, ^{230}Th). One difference between their initial model of particle cycling, however, is that total ^{234}Th was in secular equilibrium over most of the water column, contrary to many of the measurements presented here. Finally, another path of investigation to which this data may be important is the role that biominerals and lithogenic material play in transporting carbon to depth (Dunne et al., 2007; Sanders et al., 2010; Lam et al., 2011) by directly comparing particle fluxes, stocks, and composition.

The data presented in this manuscript was included in the GEOTRACES Intermediate Data Product and is available for download from the GEOTRACES Data Management Committee website (http://www.bodc.ac.uk/geotraces/data/idp2014/).

Acknowledgments

This work was generously funded by grants from the National Science Foundation (OCE-0925158) to Woods Hole Oceanographic Institution and the University of South Carolina. S. Owens was supported by a NASA Earth and Space Science Graduate Fellowship (Grant NNX10AO72H).

Thank you to the captain and crew of the R/V *Knorr* and RRS *James Cook* for their support of this work. Many thanks to the lead principal investigators of the U.S. and Dutch GEOTRACES programs, including Bob Anderson, Ed Boyle, Greg Cutter, Bill Jenkins, Hein de Baar, and Micha Rijkenberg. Thank you to the other members of the pump group, Paul Morris, Dan Ohnemus, Sylvain Rigaud, Kuanbo Zhou, Phoebe Lam, Matt Charette, and Billy Moore. A final thank you goes to two anonymous reviewers and several others who helped make this work and manuscript a reality: Pere Masque, Michiel Rutgers van der Loeff, Carl Lamborg, Dave Glover, and Mick Follows.

References

Ambar, I., Serra, N., Brogueira, M.J., Cabecadas, G., Abrantes, F., Freitas, P., Goncalves, C., Gonzalex, N., 2002. Physical, chemical, and sedimentological aspects of the Mediterranean outflow off Iberia. Deep Sea Res. Part I 49, 4163–4177.

Bacon, M.P., Rutgers van der Loeff, M.M., 1989. Removal of thorium-234 by scavenging in the bottom nepheloid layer of the ocean. Earth Planet. Sci. Lett. 92 (2), 157–164.

Baskaran, M., Santschi, P.H., Laodong, G., Bianchi, T.S., Lambert, C., 1996. ^{234}Th:^{238}U disequilibria in the Gulf of Mexico: the importance of organic matter and particle concentration. Cont. Shelf Res. 16 (3), 353–380.

Benitez-Nelson, C., Buesseler, K.O., Karl, D.M., Andrews, J., 2001a. A time-series study of particulate matter export in the North Pacific Subtropical Gyre based on Th-234: U-238 disequilibrium. Deep Sea Res. Part I 48 (12), 2595–2611.

Benitez-Nelson, C.R., Buesseler, K.O., van der Loeff, M.R., Andrews, J., Ball, L., Crossin, G., Charette, M.A., 2001b. Testing a new small-volume technique for determining ^{234}Th in seawater. J. Radioanal. Nucl. Chem. 248 (3), 795–799.

Bhat, S.G., Krishnaswamy, S., Lal, D., Rama, Moore, W.S., 1969. ^{234}Th/^{238}U ratios in the ocean. Earth Planet. Sci. Lett. 5, 483–491.

Bishop, J.K.B., Edmond, J.M., Ketten, D.R., Bacon, M.P., Silker, W.B., 1977. The chemistry, biology, and vertical flux of particulate matter from the upper 400 m of the equatorial Atlantic Ocean. Deep Sea Res. 24 (6), 511–548.

Bruland, K.W., Lohan, M.C., 2003. Controls of trace metals in seawater. In: Elderfield, H. (Ed.), The Oceans and Marine Geochemistry. Elsevier Ltd., pp. 23–47.

Buesseler, K.O., Bacon, M.P., Cochran, J.K., Livingston, H.D., 1992. Carbon and nitrogen export during the JGOFS North Atlantic Bloom Experiment estimated from ^{234}Th:^{238}U disequilibria. Deep Sea Res. Part I 39 (7-8), 1115–1137.

Buesseler, K.O., Benitez-Nelson, C.R., Moran, S.B., Burd, A., Charette, M., Cochran, J.K., Coppola, L., Fisher, N.S., Fowler, S.W., Gardner, W., Guo, L.D., Gustafsson, O., Lamborg, C., Masque, P., Miquel, J.C., Passow, U., Santschi, P.H., Savoye, N., Stewart, G., Trull, T., 2006. An assessment of particulate organic carbon to thorium-234 ratios in the ocean and their impact on the application of ^{234}Th as a POC flux proxy. Mar. Chem. 100 (3-4), 213–233.

Buesseler, K.O., Benitez-Nelson, C.R., Rutgers van der Loeff, M., Andrews, J., Ball, L., Crossin, G., Charette, M.A., 2001. An intercomparison of small- and large-volume techniques for thorium-234 in seawater. Mar. Chem. 74 (1), 15–28.
Buesseler, K.O., Boyd, P.W., 2009. Shedding light on processes that control particle export and flux attenuation in the twilight zone of the open ocean. Limnol. Oceanogr. 54 (4), 1210–1232.
Buesseler, K.O., Lamborg, C., Cai, P., Escoube, R., Johnson, R., Pike, S., Masque, P., McGillicuddy, D., Verdeny, E., 2008a. Particle fluxes associated with mesoscale eddies in the Sargasso Sea. Deep Sea Res. Part II 55 (10-13), 1426–1444.
Buesseler, K.O., Pike, S., Maiti, K., Lamborg, C.H., Siegel, D.A., Trull, T.W., 2008b. Thorium-234 as a tracer of spatial, temporal and vertical variability in particle flux in the North Pacific. Deep Sea Res. Part I 56 (7), 1143–1167.
Cai, P., Chen, W., Dai, M., Wan, Z., Wang, D., Li, Q., Tang, T., Lv, D., 2008. A high-resolution study of particle export in the southern South China Sea based on Th-234/U-238 disequilibrium. J. Geophys. Res., 113.
Charette, M.A., Buesseler, K.O., 2000. Does iron fertilization lead to rapid carbon export in the Southern Ocean? Geochem. Geophys. Geosyst. 1 (2000GC000069).
Charette, M.A., Moran, S.B., 1999. Rates of particle scavenging and particulate organic carbon export estimated using ^{234}Th as a tracer in the subtropical and equatorial Atlantic Ocean. Deep Sea Res. Part II 46 (5), 885–906.
Charette, M.A., Moran, S.B., Pike, S.M., Smith, J.N., 2001. Investigating the carbon cycle in the Gulf of Maine using the natural tracer thorium 234. J. Geophys. Res. Oceans 106 (C6), 11553–11579.
Coale, K.H., Bruland, K.W., 1987. Oceanic stratified euphotic zone as elucidated by ^{234}Th:^{238}U disequilibria. Limnol. Oceanogr. 32 (1), 189–200.
Coppola, L., Roy-Barman, M., Mulsow, S., Povinec, P., Jeandel, C., 2005. Low particulate organic carbon export in the frontal zone of the Southern Ocean (Indian sector) revealed by ^{234}Th. Deep Sea Res. Part I 52 (1), 51–68.
De Baar, H.J.W., Timmermans, K.R., Laan, P., De Porto, H.H., Ober, S., Blom, J.J., Bakker, M.C., Schilling, J., Sarthou, G., Smit, M.G., Klunder, M., 2008. Titan: a new facility for ultraclean sampling of trace elements and isotopes in the deep oceans in the international GEOTRACES program. Mar. Chem. 111 (1-2), 4–21.
Djogić, R., Sipos, L., Branica, M., 1986. Characterization of uranium (VI) in seawater. Limnol. Oceanogr. 31 (5), 1122–1131.
Dunne, J.P., Sarmiento, J.L., Gnanadesikan, A., 2007. A synthesis of global particle export from the surface ocean and cycling through the ocean interior and on the seafloor. Global Biogeochem. Cycles 21, 4.
Gardner, W.D., Richardson, M.J., Carlson, C.A., Hansell, D., Mishonov, A.V., 2003. Determining true particulate organic carbon: bottles, pumps and methodologies. Deep Sea Res. Part II 50 (3-4), 655–674.
GEOTRACES Planning Group, 2006. GEOTRACES Science Plan. Scientific Committee on Oceanic Research, Baltimore, Maryland.
German, C.R., Fleer, A.P., Bacon, M.P., Edmond, J.M., 1991. Hydrothermal scavenging at the mid-Atlantic ridge–radionuclide distributions. Earth Planet. Sci. Lett. 105 (1-3), 170–181.
Inthorn, M., Rutgers van der Loeff, M., Zabel, M., 2006. A study of particle exchange at the sediment-water interface in the Benguela upwelling area based on Th-234/U-238 disequilibrium. Deep Sea Res. Part I 53, 1742–1761.
Kadko, D., 1996. Radioisotopic studies of submarine hydrothermal vents. Rev. Geophys. 34 (3), 349–366.
Kadko, D., Feely, R., Massoth, G., 1994. Scavenging of Th-234 and phosphorus removal from the hydrothermal effluent plume over the North Cleft segment of the Juan de Fuca Ridge. J. Geophys. Res. 99, 5017–5024.
Lam, P.J., Doney, S.C., Bishop, J.K.B., 2011. The dynamic ocean biological pump: insights from a global compilation of particulate organic carbon, $CaCO_3$, and opal concentration profiles from the mesopelagic. Global Biogeochem. Cycles 25, GB3009.
Lam, P.J., Ohnemus, D., Auro, M., 2015. Size fractionated major particle composition and mass from the US GEOTRACES North Atlantic Zonal Transect. Deep Sea Res. Part II 116, 303–320. http://dx.doi.org/10.1016/j.dsr2.2014.11.020.
Le Moigne, F., Henson, S.A., Sanders, R., Madsen, E., 2013. Global database of surface ocean particulate organic carbon export fluxes diagnosed from the Th-234 technique. Earth Syst. Sci. Data 5, 295–304.
MacIntyre, S., Alldredge, A.L., Gotschalk, C.C., 1995. Accumulation of marine snow at density discontinuities in the water column. Limnol. Oceanogr. 40 (3), 449–468.
Maiti, K., Benitez-Nelson, C.R., Buesseler, K.O., 2010. Insights into particle formation and remineralization using the short-lived radionuclide, thorium-234. Geophys. Res. Lett., 37.
Maiti, K., Buesseler, K.O., Pike, S.M., Benitez-Nelson, C.R., Cai, P., Weifang, C., Cochran, J.K., Dai, M., Dehairs, F., Gasser, B., Kelly, R.P., Masqué, P., Miller, L.A., Miquel, J.C., Moran, S.B., Morris, P.J., Peine, F., Planchon, F., Renfro, A., Rutgers van der Loeff, M., Santschi, P.H., Turnewitsch, R., Waples, J.T., Xu, C., 2012. Intercalibration studies of short-lived thorium-234 in the water column and marine particles. Limnol. Oceanogr.: Methods 10, 631–644.
Marchal, O., Lam, P.J., 2012. What can paired measurements of Th isotope activity and particle concentration tell us about particle cycling in the ocean? Geochim. Cosmochim. Acta 90, 126–148.
Marra, J.F., Lance, V.P., Vaillancourt, R.D., Hargreaves, B.R., 2014. Resolving the ocean's euphotic zone. Deep Sea Res. Part I 83, 45–50.
Mittelstaedt, E., 1991. The ocean boundary along the northwest African coast: circulation and oceanographic properties at the sea surface. Prog. Oceanogr. 26, 307–355.
Moran, S.B., Charette, M.A., Pike, S.M., Wicklaund, C.A., 1999. Differences in seawater particulate organic carbon concentration in samples collected using small- and large-volume methods: the importance of DOC adsorption to the filter blank. Mar. Chem. 67 (1-2), 33–42.
Morris, P.J., Charette, M.A., Buesseler, K.O., Lam, P.J., Auro, M., Henderson, P., Manganini, S., Murray, J., Ohnemus, D., Owens, S.A., Pike, S.M., Zhou, K., 2011. The Collection of Trace Elements and Isotopes Using a Newly Modified In situ Pump–Radium as a Case Study. Liege Colloquium, Liege, Belgium.
Morris, P.J., Charette, M.A., Jenkins, W.J., Henderson, G.M., Moore, W.S., 2012. Radium-derived mixing rates in the North Atlantic. In: Fourth International Ra–Rn Workshop, Rhode Island, USA.
Owens, S.A., Buesseler, K.O., Sims, K.W.W., 2011. Re-evaluating the U-238-salinity relationship in seawater: implications for the U-238/Th-234 disequilibrium method. Mar. Chem. 127, 31–39.
Pike, S.M., Buesseler, K.O., Andrews, J., Savoye, N., 2005. Quantification of ^{234}Th recovery in small volume sea water samples by inductively coupled plasma mass spectrometry. J. Radioanal. Nucl. Chem. 263 (2), 355–360.
Planchon, F., Cavagna, A.J., Cardinal, D., Andre, L., Dehairs, F., 2012. Late summer particulate organic carbon export and twilight zone remineralisation in the Atlantic sector of the Southern Ocean. Biogeosci. Discuss. 9, 3423–3477.
Resplandy, L., Martin, A.P., Le Moigne, F., Martin, P., Aquilina, A., Mémery, M., Lévy, M., Sanders, R., 2012. How does dynamical spatial variability impact Th-234 derived estimates of organic export? Deep Sea Res. Part I.
Rutgers van der Loeff, M., Cai, P.H., Stimac, I., Bracher, A., Middag, R., Klunder, M.B., van Heuven, S.M.A.C., 2011. Th-234 in surface waters: distribution of particle export flux across the Antarctic Circumpolar Current and in the Weddell Sea during the GEOTRACES expedition ZERO and DRAKE. Deep Sea Res. Part II 58 (25-26), 2749–2766.
Rutgers van der Loeff, M.M., Meyer, R., Rudels, B., Rachor, E., 2002. Resuspension and particle transport in the benthic nepheloid layer in and near Fram Strait in relation to faunal abundances and Th-234 depletion. Deep Sea Res. Part I 49 (11), 1941–1958.
Sanders, R., Morris, P.J., Poulton, A.J., Stinchcombe, M.C., Charalampopoulou, A., Lucas, M.I., Thomalla, S.J., 2010. Does a ballast effect occur in the surface ocean? Geophys. Res. Lett. 37, L08602.
Santschi, P.H., Guo, L., Walsh, I.D., Quigley, M.S., Baskaran, M., 1999. Boundary exchange and scavenging of radionuclides in continental margin waters of the Middle Atlantic Bight: implications for organic carbon fluxes. Cont. Shelf Res. 19 (5), 609–636.
Savoye, N., Benitez-Nelson, C., Burd, A.B., Cochran, J.K., Charette, M., Buesseler, K.O., Jackson, G.A., Roy-Barman, M., Schmidt, S., Elskens, M., 2006. ^{234}Th sorption and export models in the water column: a review. Mar. Chem. 100 (3-4), 234–249.
Savoye, N., Buesseler, K.O., Cardinal, D., Dehairs, F., 2004. Th-234 deficit and excess in the Southern Ocean during spring 2001: particle export and remineralization. Geophys. Res. Lett. 31 (12) (art. no.-L12301).
Schmidt, S., 2006. Impact of the Mediterranean Outflow Water on the particle dynamics in intermediate waters of the Northeast Atlantic as revealed by Th-234 and Th-228. Mar. Chem. 100, 289–298.
Sutherland, K.R., Madin, L.P., Stocker, R., 2010. Filtration of submicrometer particles by pelagic tunicates. Proc. Natl. Acad. Sci. U.S.A. 107 (34), 15129–15134.
Sweeney, E.N., McGillicuddy Jr., D.J., Buesseler, K.O., 2003. Biogeochemical impacts due to mesoscale eddy activity in the Sargasso Sea as measured at the Bermuda Atlantic Time-series Study (BATS). Deep Sea Res. Part II 50, 3017–3039.
Thomalla, S., Turnewitsch, R., Lucas, M., Poulton, A., 2006. Particulate organic carbon export from the North and South Atlantic gyres: the ^{234}Th/^{238}U disequilibrium approach. Deep Sea Res. Part II 53 (14-16), 1629–1648.
Turnewitsch, R., Reyss, J.-L., Nycander, J., Waniek, J., Lampitt, R.S., 2008. Internal tides and sediment dynamics in the deep sea—evidence from radioactive Th-234/U-238 disequilibria. Deep Sea Res. Part I 55, 1727–1747.
Turnewitsch, R., Springer, B.M., 2001. Do bottom mixed layers influence Th-234 dynamics in the abyssal near-bottom water column? Deep Sea Res. Part I 48 (5), 1279–1307.
Waples, J.T., Benitez-Nelson, C., Savoye, N., Rutgers van der Loeff, M., Baskaran, M., Gustafsson, O., 2006. An introduction to the application and future use of ^{234}Th in aquatic systems. Mar. Chem. 100 (3-4), 166–189.
Weinstein, S.E., Moran, S.B., 2005. Vertical flux of particulate Al, Fe, Pb, and Ba from the upper ocean estimated from Th-234/U-238 disequilibria. Deep Sea Res. Part I 52, 1477–1488.